

[Click here to view linked References](#)

1

# Epigenetic alterations in TRAMP mice: genomic DNA methylation profiling using MeDIP-seq

Wenji Li<sup>a,b,1</sup>, Ying Huang<sup>a,b,c,1</sup>, Davit Sargsyan<sup>a,b,c</sup>, Tin Oo Khor<sup>a,b</sup>, Yue Guo<sup>a,b,c</sup>, Limin Shu<sup>a,b</sup>, Anne Yuqing Yang<sup>a,b,c</sup>, Chengyue Zhang<sup>a,b,c</sup>, Ximena Paredes-Gonzalez<sup>a,b,c</sup>, Michael Verzi<sup>d</sup>, Ronald P Hart<sup>e</sup>, and Ah-Ng Tony Kong<sup>a,b,\*</sup>

<sup>a</sup>Center for Cancer Prevention Research, Ernest Mario School of Pharmacy, The State University of New Jersey, Piscataway, NJ 08854, USA.

<sup>b</sup>Department of Pharmaceutics, Ernest Mario School of Pharmacy, The State University of New Jersey, Piscataway, NJ 08854, USA.

<sup>c</sup>Graduate Program in Pharmaceutical Sciences, Ernest Mario School of Pharmacy, The State University of New Jersey, Piscataway, NJ 08854, USA.

<sup>d</sup>Department of Genetics, The State University of New Jersey, Piscataway, NJ 08854, USA.

<sup>°</sup>Department of Cell Biology and Neuroscience, Rutgers, The State University of New Jersey, Piscataway, NJ 08854, USA.

<sup>1</sup>Equal contribution

\*Correspondence should be addressed to:  
Professor Ah-Ng Tony Kong  
Rutgers, The State University of New Jersey  
Ernest Mario School of Pharmacy, Room 228  
160 Frelinghuysen Road,  
Piscataway, NJ 08854, USA  
Email: [kongt@pharmacy.rutgers.edu](mailto:kongt@pharmacy.rutgers.edu)  
Phone: 848-445-6369/8  
Fax: 732-445-3134

Color figures are intended for reproduction in color on the Web and in black-and-white in print.

1  
2  
3  
4       33       This work was supported in part by institutional funds and by R01AT007065 from the National  
5  
6       34       Center for Complementary and Alternative Medicines (NCCAM) and the Office of Dietary  
7  
8       35       Supplements (ODS).  
9  
10      36  
11  
12  
13      37       Abbreviations:  
14  
15      38       TRAMP-Transgenic adenocarcinoma of the mouse prostate  
16  
17      39       MeDIP - Methylated DNA immunoprecipitation  
18  
19      40       IPA- Ingenuity® pathway analysis  
20  
21      41       CREB1-Cyclic AMP (cAMP) response element-binding protein 1  
22  
23      42       HDAC2- Histone deacetyltransferase 2  
24  
25      43       GSTP1-Glutathione S-transferase 1  
26  
27      44       UBC-Ubiquitin C  
28  
29      45  
30  
31      46       Keywords: MeDIP-seq, Epigenetics, DNA methylation, TRAMP, Prostate Cancer  
32  
33      47  
34  
35  
36  
37  
38  
39  
40  
41  
42  
43  
44  
45  
46  
47  
48  
49  
50  
51  
52  
53  
54  
55  
56  
57  
58  
59  
60  
61  
62  
63  
64  
65

2

**Abstract**

**Purpose:** We investigated the genomic DNA methylation profile of prostate cancer in transgenic adenocarcinoma of the mouse prostate (TRAMP) cancer model and to analyze the crosstalk among targeted genes and the related functional pathways.

**Methods:** Prostate DNA samples from 24-week-old TRAMP and C57BL/6 male mice were isolated. The DNA methylation profiles were analyzed by methylated DNA immunoprecipitation (MeDIP) followed by next-generation sequencing (MeDIP-seq). Canonical pathways, diseases & function and network analyses of the different samples were then performed using the Ingenuity® Pathway Analysis (IPA) software. Some genes were randomly selected for validation using Methylation Specific Primers (MSP) and qPCR.

**Results:** TRAMP mice undergo extensive aberrant CpG hyper- and hypo-methylation. There were 2,147 genes with a significant ( $\log_2$ -fold change  $\geq 2$ ) change in CpG methylation peaks between the two groups, as mapped by the IPA software. Among these genes, the methylation of 1,105 and 1,042 genes was significantly decreased and increased, respectively, in TRAMP prostate tumors. The top associated disease identified by IPA was adenocarcinoma; however, the CREB-, HDAC2-, GSTP1- and UBC-related pathways showed significantly altered methylation profiles based on the canonical pathway and network analyses. MSP and qPCR results of randomly selected genes corroborated with MeDIP-seq.

**Conclusions:** This is the first MeDIP-seq with IPA analysis of the TRAMP model to provide novel insight into the genome-wide methylation profile of prostate cancer. Studies on epigenetics, such as DNA methylation, will potentially provide novel avenues and strategies for further development of biomarkers targeted for treatment and prevention approaches for prostate cancer.

## Introduction

Prostate cancer is the second most common cancer of men (914 000 new cases, 13.8% of the total) and the fifth most common among all cancers [1]. In the United States, prostate cancer is the most common male cancer subtype, apart from non-melanoma skin cancer [2]. Prostate cancer is a clinically heterogeneous disease with marked variability in patient outcomes [3]. Early detection, accurate prediction and successful management of prostate cancer represent some of the most challenging and controversial issues [4]. Interestingly, epigenetic changes are hallmarks of prostate cancer, among which DNA methylation is the most frequently studied [5].

Epigenetic changes include DNA methylation, histone modification, and posttranslational gene regulation by micro-RNAs (miRNAs) [6]. Among these, DNA methylation has been well studied, and aberrant DNA methylation patterns are a characteristic feature of cancer [7, 8]. The first reported epigenetic changes in human cancer were DNA methylation losses [9]. Since then, genomic hypomethylation has been found to be associated with multiple cancer types [10, 11]. In addition, hypermethylation of CpG islands (CGIs) at promoters of tumor suppressor genes, homeobox genes and other sequences are other consistent epigenetic features of cancer [12]. CGI methylator-phenotype (CIMP) tumors have been identified in many cancers, including oral cancer [13], colorectal cancer [14] and colon cancer [15]. Therefore, it is worthwhile to profile the global DNA methylation changes between cancer models and controls to elucidate the mechanisms of carcinogenesis.

The transgenic adenocarcinoma of the mouse prostate (TRAMP) model closely represents the pathogenesis of human prostate cancer because male TRAMP mice spontaneously develop autochthonous prostate tumors following the onset of puberty [16] and it specifically induces transgene expression in the prostate, displays distant organ metastases and it has castration-resistant properties [17]. DNA methylation in the TRAMP model has been widely studied *in vitro* and *in vivo*, resulting in the discovery of the methylated markers Nrf2 [18], MGMT[19], GSTP1 [20], 14-3-3 $\sigma$  [21], and KLF6 [22].

However, only Shannon et al have compared global methylation alteration among TRAMP and WT mice [23]. Systemic comparisons and analyses of the genomic methylation status of prostate cancer

models and normal controls are needed to determine the underlying interactions between these target genes and to discover new biomarkers. We are the first to perform methylated DNA immunoprecipitation (MeDIP) coupled with next-generation sequencing (MeDIP-seq) followed by Ingenuity® Pathway Analysis (IPA) studies to investigate the crosstalk among important genes and to analyze overlapping functional pathways by comparing the whole genomic DNA methylation patterns between the TRAMP model and controls.

## Materials and methods

### Genomic DNA extraction from TRAMP and C57BL/6 male mice

The breeding of TRAMP mice were followed our previous publication [24, 25]. Briefly, female hemizygous C57BL/TGN TRAMP mice, line PB Tag 8247NG (Jackson Laboratory, Bar Harbor, ME), were bred with the same genetic background male C57BL/6 mice (Jackson Laboratory, Bar Harbor, ME). Identity of transgenic mice was established by PCR-based DNA genotyping using the primers suggested by The Jackson Laboratory as we previously described [24, 25]. F1 (first generation from cross breeding) or F2 (second generation from cross breeding) male TRAMP mice were used for the studies. Mice were housed in cages containing wood-chip bedding in a temperature-controlled room (20–22°C) with a 12-h-light/dark cycle and a relative humidity of 45–55% at Rutgers Animal Care Facility. All animals received water and food *ad libitum* until sacrifice (24 weeks of age) by carbon dioxide euthanasia. The study was performed using an IACUC-approved protocol at Rutgers University. Mice were weighted and evaluated in the overall health twice weekly during all the study. Presences of palpable tumor, metastases, genitourinary (GU) apparatus weight were evaluated upon necropsy and prostate intraepithelial neoplasia lesions (evaluated by H&E staining) were monitored in the TRAMP group (data not shown). Prostate samples from three 24-week-old TRAMP and three 24 weeks old C57BL/6 mice (maintained under similar conditions) were randomly selected out. A DNeasy Kit (Qiagen, Valencia, CA, USA) was used to extract the genomic DNA (gDNA) from prostate samples of three 24-week-old male TRAMP mice and three age-matched C57BL/6 male mice according to the manufacturer's protocol. After extraction and

1  
2  
3  
4 124 purification, the gDNA samples were electrophoresed on an agarose gel, and the OD ratios were  
5  
6 125 measured to confirm the purity and concentrations of the gDNA prior to fragmentation by Covaris  
7  
8 126 (Covaris, Inc., Woburn, MA USA). The fragmented gDNA was then evaluated for size distribution and  
9  
10 127 concentration using an Agilent Bioanalyzer 2100 and a NanoDrop spectrophotometer.  
11  
12  
13 128  
14  
15 129 **MeDIP-seq measurement**  
16  
17 130 Following the manufacturer's instructions, MeDIP was performed to analyze genome-wide  
18  
19 131 methylation using the MagMeDIP Kit from Diagenode (Diagenode Inc., Denville, NJ, USA). Methylated  
20  
21 132 DNA was separated from unmethylated fragments by immunoprecipitation with a 5-methylcytidine  
22  
23 133 monoclonal antibody that was purchased from Eurogentec (Eurogentec S.A., Seraing, Belgium). Illumina  
24  
25 134 libraries were then created from the captured gDNA using NEBNext reagents (New England Biolabs,  
26  
27 135 Ipswich, MA, USA). Enriched libraries were evaluated for size distribution and concentration using an  
28  
29 136 Agilent Bioanalyzer 2100, and the samples were then sequenced on an Illumina HiSeq2000 machine,  
30  
31 137 which generated paired-end reads of 90 or 100 nucleotides (nt). The results were analyzed for data quality  
32  
33 138 and exome coverage using the platform provided by DNAnexus (DNAnexus, Inc., Mountain View, CA,  
34  
35 139 USA). The samples were sent to Otogenetics Corp. (Norcross, GA) for Illumina sequencing and  
36  
37 140 alignment with the genome. The resulting BAM files were downloaded for analysis.  
38  
39  
40  
41

42 141 Modified from the Trapnell method, the MeDIP alignments were compared with control sample  
43  
44 142 alignments using Cuffdiff 2.0.2 with no length correction [26]. Briefly, a list of overlapping regions of  
45  
46 143 sequence alignment that were common to both the immunoprecipitated and control samples was created  
47  
48 144 and used to determine the quantitative enrichment of the MeDIP samples over the control samples using  
49  
50 145 Cuffdiff; statistically significant peaks (reads) at a 5% false discovery rate (FDR) and a minimum 4-fold  
51  
52 146 difference, as calculated using the Cummerbund package in R, were selected (Trapnell et al., 2012).  
53  
54 147 Sequencing reads were matched with the adjacent annotated genes using ChIPpeakAnno [27], and the  
55  
56 148 uniquely mapped reads were used to compare the differences between TRAMP and wild-type mice.  
57  
58  
59  
60 149  
61  
62  
63  
64  
65

1  
2  
3  
4 150 **Canonical pathways, diseases & function and network analysis by IPA**

5  
6 151 Genes selected from the MeDIP-seq experiment based on significant increased or decreased fold  
7 changes ( $\log_2$ -fold change  $\geq 2$ ) in the methylation pattern were analyzed (based on the p-values; TRAMP  
8 vs. control) using IPA 4.0 When using IPA (IPA 4.0, Ingenuity Systems, [www.ingenuity.com](http://www.ingenuity.com)), the  
9 pathway enrichment p-value is calculated using the right-tailed Fisher Exact Test. A smaller *p*-value  
10 indicated that the association was less likely to be random and more likely to be significant. In general,  
11 values of 0.05 (for *p*-value) or 1.30 (for  $-\log_{10}P$ ) were set as the thresholds. P-values less than 0.05 or  $-\log_{10}P$   
12 more than 1.30 were considered to be statistically significant, non-random associations. IPA  
13 utilized gene symbols to identify neighboring enriched methylation peaks using ChIPpeakAnno for all of  
14 the analyses. Using IPA, 2147 genes in the TRAMP group that showed a  $\log_2$ -fold change  $\geq 2$  compared  
15 with the control group were mapped. Based on these fold changes, IPA identified the canonical pathways,  
16 biological functions/related diseases and networks that were closely related to the TRAMP model.  
17  
18  
19  
20  
21  
22  
23  
24  
25  
26  
27  
28  
29  
30  
31 162  
32  
33 163 **MeDIP-seq data validation via Methylation-specific PCR (MSP)**  
34  
35 164 Genomic DNA was extracted from six prostate samples (three from TRAMP mice and three from  
36 normal C57BL/6 mice) using the AllPrep DNA/RNA/Protein Mini Kit (Qiagen, Valencia, CA, USA).  
37  
38 165 Then 500 ng of genomic DNA was subjected to bisulfite conversion with an EZ DNA Methylation-Gold  
39 Kit (Zymo Research Corp., Orange, CA) according to the manufacturer's instructions as described  
40 previously [28]. The converted DNA was amplified by PCR using EpiTaq HS DNA polymerase  
41 (Clontech Laboratories Inc, Mountain View, CA 94043, USA). According to MeDIP-seq results, four  
42 genes (2 with increased methylation and 2 with decreased methylation), Dync1i1, Slc1a4, Xrcc6bp1 and  
43 TTR, were randomly selected for MSP validation. The primers' sequences for the methylated reactions  
44 (MF and MR) and for the unmethylated reactions (UF and UR) and band size of products are listed in  
45 Table 1. The amplification products were separated by agarose gel electrophoresis and visualized by  
46 ethidium bromide staining using a Gel Documentation 2000 system (Bio-Rad, Hercules, CA, USA). The  
47  
48  
49  
50  
51  
52  
53  
54  
55  
56  
57  
58 174  
59  
60  
61  
62  
63  
64  
65

bands were semi-quantitated by densitometry using ImageJ (Version 1.48d; NIH, Bethesda, Maryland, USA).

### Validation of selected gene expression by Real-time RT-PCR

Total RNA was extracted from six prostate samples (three from TRAMP mice and three from normal C57BL/6 mice) using the AllPrep DNA/RNA/Protein Mini Kit (Qiagen, Valencia, CA, USA). First-strand cDNA was synthesized from total RNA using a SuperScript III First-Strand Synthesis System (Invitrogen, Grand Island, NY) according to the manufacturer's instructions. mRNA expression levels were determined using first strand cDNA as the template by quantitative real-time PCR (qPCR) with Power SYBR Green PCR Master Mix (Applied Biosystems, Carlsbad, CA) in an ABI7900HT system. HNMT, Dync1i1, SLC1A4, Cryz and TTR were randomly selected to compare mRNA expression among WT and TRAMP mice prostate samples. The primers' sequences for HNMT, Dync1i1, SLC1A4, Cryz, TTR and β-Actin are listed in Table 2.

## Results

### MeDIP-seq results comparison

A primary goal of the study was to identify aberrantly methylated genes and discover the related functions and pathways that might mediate the development of prostate cancer. To accomplish this objective in an unbiased manner, the MeDIP-seq results were analyzed using IPA. The first objective was to compare the total number of molecules with altered methylation in prostate samples of TRAMP mice to that of normal mice. Prostate samples were collected from the TRAMP and C57BL/6 mice, gDNA was isolated, and whole-genome DNA methylation analysis was performed using the described MeDIP-seq method. The results were analyzed in a paired manner, comparing the prostate tissue samples for each model. For the control, 16 509 344 (80.8%) mapped reads and 3 921 684 (19.2%) non-mapped reads, for a total of 20 431 028 reads, were obtained. For the TRAMP mice, 12 097 771 (82.3%) mapped reads and 2 609 269 (17.7%) non-mapped reads, for a total of 14 707 040 reads, were obtained (Fig. 1A). After

1  
2  
3  
4 201 identification and mapping to the library, the identified methylated regions (peaks) of the given genes  
5  
6 202 were compared between the TRAMP and control mice, and IPA was used to identify the genes with  
7  
8 203 significantly altered methylation in the TRAMP mice compared with the controls ( $p<0.05$  or –  
9  
10 204  $\log_{10}P>1.30$ , and  $\log_2$ -fold change  $\geq 2$ ).  
11  
12

13 205 According to the IPA setting , the  $p$ -value for a given process annotation was calculated by  
14  
15 206 considering (1) the number of focus genes that participated in the process and (2) the total number of  
16 genes that are known to be associated with that process in the selected reference set. The more focus  
17  
18 207 genes that are involved, the more likely the association is not due to random chance, resulting in a more  
19  
20 208 significant p-value (larger  $-\log_{10}P$ -value). Altogether, 2147 genes between the two groups showed a  
21  
22 209 significant change ( $\log_2$ -fold change  $\geq 2$ ) in methylated peaks. Compared with the control, significantly  
23  
24 210 decreased methylation of 1105 genes and significantly increased methylation of 1042 genes were  
25  
26 211 observed in TRAMP (Fig. 1B). The top 50 genes with increased methylation (Table 3) or decreased  
27  
28 212 methylation (Table 4) located in promoter region, gene body or downstream of the gene were highlighted  
29  
30 213 based on the  $\log_2$ -fold change, from highest to lowest; all  $p$ -values were less than 0.05. We also plotted  
31  
32 214 the top 100 decreased or increased (Log2-fold Change) methylated genes comparing with TRAMP to WT  
33  
34 215 in different regions by MeDIP analysis, ranked by alphabet (Fig 2).  
35  
36 216  
37  
38 217 These results demonstrate a fundamental difference in the global pattern of gene methylation  
39  
40 218 between the TRAMP prostate tumor and control prostate tissue. The potential impact of this difference  
41  
42 219 was further assessed using IPA by analyzing the canonical pathways, diseases and functions, and  
43  
44 220 networks related to these methylation changes.  
45  
46  
47 221  
48  
49 222  
50  
51 223 **MeDIP-seq data validation by MSP**  
52  
53 224 According to the MeDIP-seq results, two genes with increased methylation (TRAMP vs WT),  
54  
55 225 DYNC1I1 and SLC1A4, and two genes with decreased methylation (TRAMP vs WT), XRCC6BP1 and  
56  
57 226 TTR were selected randomly to carry out MSP to validate the MeDIP-seq data. MSP results indicated a  
58  
59 similar trend in agreement with the MeDIP-seq results.  
60  
61  
62  
63  
64  
65

1  
2  
3  
4 227 The results showed, in *Dync1i1* and *Slc1a4* genes, the relative density of M-MSP (methylated  
5  
6 MSP) to that of U-MSP (unmethylated MSP) in TRAMP group were increased, which indicated that the  
7  
8 CpG sites of these genes were hypermethylated in TRAMP mice (Fig. 3). Similarly, in *Xrcc6bp1* and  
9  
10 TTR, the relative density of M-MSP to that of U-MSP in TRAMP group was decreased, which indicated  
11  
12 that the CpG sites of these genes were hypomethylated in TRAMP mice (Fig. 3).

13 231  
14  
15 232  
16  
17 233 **qPCR Validation of selected gene expression**

18 234 When mRNA levels were measured by qPCR, the relative expression levels of CRYZ, DYNC1I1,  
19  
20 HNMT, SLC1A4 and TTR in TRAMP group were 0.62, 1.90, 0.15, 0.15 and 9.05 fold compared with  
21  
22 WT (Fig. 4). Among these, TTR expression was increased by 9.05-fold over WT, which agreed with  
23  
24 results reported by Wang et al. that expression levels of TTR were significantly higher in Prostate cancer  
25  
26 tissue than in normal and benign prostate hyperplasia tissue [29]. When comparing mRNA expression  
27  
28 and Methylation validation results, reciprocal relationships were found in TTR in TRAMP, which  
29  
30 indicated decreased methylation in promoter region but increased gene expression when comparing with  
31  
32 WT. In contrast, DNA methylation in the gene body or downstream may or may not follow a reciprocal  
33  
34 relationship with gene expression as described in the findings of Yi-Zhou Jiang et.al. [30]. It is expected  
35  
36 that individual genes may be differentially affected by CpG methylation and that only global analysis  
37  
38 would be expected to reveal overall patterns likely to emerge.

39 243  
40 244  
41  
42 245  
43  
44 246 **Canonical pathway, diseases & functions and network analyses by IPA**

45  
46  
47 247 To ascertain the significance of the methylation changes, the 2147 genes with a greater than  $\log_2$ -  
48  
49 fold change in methylation were analyzed using the IPA software package. When using IPA, canonical  
50  
51 pathways, which are based on the literature and are generated prior to data input, are the default settings.  
52  
53 249 These pathways do not change upon data input and have a directionality-linked list of interconnected  
54  
55 nodes. By contrast, networks are generated *de novo* based upon input data, lack directionality and contain  
56  
57 molecules that are involved in a variety of canonical pathways.

1  
2  
3  
4 253 The genes within the canonical pathways were ranked by the possibility parameter, i.e., the –  
5

6 254  $\log_{10}(P)$  value in the corresponding pathway, and are presented in Table 5. The CREB1 gene, which is  
7 involved the neuropathic pain signaling pathway, was ranked first. The top networks ranked based on  
8 their ratios of methylated gene/total gene are listed in Table 6. Of the networks, the histone  
9 deacetyltransferase 2 (HDAC2)-related, tissue morphology, embryonic development, and organ  
10 development network was ranked first (Table 6). Among the networks, the cancer-related networks  
11 accounted for the majority (15/25) (Table 6), which indicates that the great difference between the  
12 TRAMP and control lies in organ development and cancer development.  
13

14 261 Diseases & functions refer to the most likely linked diseases or functions based on statistics.  
15

16 262 Similar to the network analysis, for the most associated disease based on the ranking of  $-\log_{10}P$ , cancer,  
17 gastrointestinal disease, organismal abnormalities, reproductive system disease and dermatological  
18 diseases were ranked within the top 5 (Fig. 5A). Of all cancer subtypes, adenocarcinoma ranked first (Fig.  
19 264 5B), which was consistent with the TRAMP model, which is a model for prostate adenocarcinoma.  
20 265  
21  
22 266  
23  
24 267  
25  
26  
27  
28  
29  
30  
31  
32  
33  
34  
35  
36  
37  
38  
39  
40  
41  
42  
43  
44  
45  
46  
47  
48  
49  
50  
51  
52  
53  
54  
55  
56  
57  
58  
59  
60  
61  
62  
63  
64  
65

## Discussion

268 **Useful canonical pathway analysis will provide further understanding of disease and information  
269 for the development of new therapeutic targets.**

270 As shown in Fig. 6, the genes with significantly altered methylation in the top canonical pathway  
271 was the neuropathic pain signaling pathway, as mapped by IPA. This finding is consistent with  
272 Chiaverotti's finding indicating that the most common malignancy in TRAMP is of neuroendocrine origin  
273 [31]. Table 7 lists the genes involved in this pathway that exhibited modified methylation. Among these,  
274 methylation of the cyclic AMP (cAMP) response element-binding protein 1 (CREB1) gene was found to  
275 be decreased by 2.274-fold ( $\log_2$ ) by MeDIP-seq in TRAMP.

276 CREB was first found to be closely related to cellular proliferation, differentiation and adaptive  
277 responses in the neuronal system [32, 33]. Subsequently, increasing evidence revealed that CREB is  
278 directly involved in the oncogenesis of a variety of cancers by regulating the immortalization and

1  
2  
3  
4 279 transformation of cancer cells. [34, 35].  
5

6 280 CREB is also found to modulate other carcinogenesis pathways. S100P is a calcium-binding  
7 protein that is associated with cancer, and functional analysis of the S100P promoter identified SMAD,  
8 STAT/CREB and SP/KLF binding sites as key regulatory elements in the transcriptional activation of the  
9 S100P gene in cancer cells [36]. *Homo sapiens* lactate dehydrogenase c (hLdhc) was reported to be  
10 expressed in a wide spectrum of tumors, including prostate cancers, and this expression was shown to be  
11 regulated by transcription factor Sp1 and CREB as well as promoter CpG island (CGI) methylation [37].  
12  
13 283 Decreased prostate tumorigenicity was found to be correlated with decreased expression of CREB and its  
14 targets, including Bcl-2 and cyclin A1 [38].  
15  
16

17 288 Clinically, overexpression and overactivation of CREB was observed in cancer tissues from  
18 patients with prostate cancer, breast cancer, non-small-cell lung cancer and acute leukemia, whereas  
19 down-regulation of CREB in several distinct cancer cell lines resulted in the inhibition of cell  
20 proliferation and induction of apoptosis [39].  
21  
22

23 292 All of these data indicate that CREB is highly associated with cancer therapy. Our study  
24 demonstrated that CREB gene methylation is significantly decreased in the TRAMP model, which  
25 suggests a new approach to prostate cancer prevention and therapy.  
26  
27

28 295  
29 296 **Novel networks involving the methylation of target genes could provide new insights for prostate**  
30 **cancer.**  
31  
32

33 298 Compared with the canonical pathways, networks are generated *de novo* based upon input data  
34 and are able to more flexibly reveal the interactions of altered genes and functions. As it is impossible to  
35 analyze all networks listed in Table 6, four interesting networks were elaborated below (the higher the  
36 score is, the more genes with altered methylation are involved in the network). Among all these networks,  
37 many genes are known to be highly associated with tumor onset and progression, however, our insight  
38 into their methylation status alteration would reveal novel biomarkers for prostate tumorigenesis.  
39  
40

41 304 **HDAC2-related network (Score=38):** The top network identified by IPA, was the HDAC2-related  
42  
43  
44  
45  
46  
47  
48  
49  
50  
51  
52  
53  
54  
55  
56  
57  
58  
59  
60  
61  
62  
63  
64  
65

1  
2  
3  
4 305 tissue morphology, embryonic development and organ development network (Table 6, Fig. 7A). In this  
5 network, the HDAC2 gene, a key member of HDAC, exhibited 3.274-fold (log2) decreased methylation  
6 in TRAMP. HDACs are responsible for the removal of acetyl groups from histones and play important  
7 roles in modulating the epigenetic process by influencing the expression of genes encoded by DNA bound  
8 to a histone molecule [40]. HDAC inhibitors have also been shown to reduce colonic inflammation [41],  
9 inhibit cell proliferation, and stimulate apoptosis, and these inhibitors represent a novel class of  
10 therapeutic agents with antitumor activity that are currently in clinical development [42, 43]. By  
11 upregulating histone H3 acetylation and p21 gene expression, long-term treatment with MS-275, an  
12 HDAC inhibitor, attenuated the progression of prostate cancer *in vitro* and *in vivo* [44]. Another HDAC  
13 inhibitor, OSU-HDAC42, also showed a chemoprevention effect on prostate tumor progression in the  
14 TRAMP model [45]. Our data suggest that the altered methylation of HDAC (3.274 Log2-fold decrease)  
15 might be a novel, interesting target for prostate cancer treatment. Based on our MeDIP-seq results, the  
16 methylation of histamine N-methyltransferase (HNMT) in this network was increased by 3.703-fold  
17 (Log2). In addition, based on our qPCR analysis, HNMT gene expression was reduced by 6.67-fold,  
18 which supports the likelihood of a role of HNMT in prostate cancer. However, although HNMT has been  
19 demonstrated to be associated with breast cancer [46] and liver cancer [47], little is known about its  
20 potential role in prostate cancer, making it another potential novel marker.  
21

22                   Glutathione S-transferase 1 (GSTP1)-related network (Score=16): GSTP1 expression is  
23 inactivated in prostate cancers [48-50], and this inactivation is associated with hypermethylation of  
24 GSTP1 CpG islands [49, 50]. Clinically, higher GSTP1 promoter methylation was found to be  
25 independently associated with the risk of prostate cancer [51]; therefore, the detection of hypermethylated  
26 GSTP1 in urine and semen samples can be a diagnostic marker of prostate cancer [52]. We also found that  
27 methylation of GSTP1 was an important factor involved in prostate cancer development. Interestingly,  
28 based on our data, the methylation of the GSTP1 gene was decreased 2.274-fold (log2) in TRAMP. Fig.  
29 7B demonstrates the decreased methylation of GSTP1. Based on comparisons of prostate samples from  
30 TRAMP and strain-matched WT mice, Mavis CK et al. showed that promoter DNA hypermethylation  
31  
32  
33  
34  
35  
36  
37  
38  
39  
40  
41  
42  
43  
44  
45  
46  
47  
48  
49  
50  
51  
52  
53  
54  
55  
56  
57  
58  
59  
60  
61  
62  
63  
64  
65

331 does not appear to drive GST gene repression in TRAMP primary tumors [20]. The above results support  
332 our finding that the methylation status of GSTP1 may differ in humans. Dynein cytoplasmic 1  
333 intermediate chain 1 (DYN1I1), which was also in the network, exhibited a 4.926-fold (Log2) increase  
334 in methylation. In qPCR analysis, it indicates a 1.9-fold increase in gene expression. Although DYN1I1  
335 is significantly up-regulated in liver tumors [53] but not in prostate tumors, our findings suggest that it  
336 may be the next useful prostate cancer biomarker.

337 Ubiquitin C (UBC)-related network (Score=16): Another interesting network was found  
338 surrounding the UBC gene (Fig. 7C); however, UBC itself was not identified by MeDIP-seq. The  
339 methylation of solute carrier family 1 member 4 (SLC1A4) and crystallin zeta (CRYZ) was highly up-  
340 regulated (3.807 and 3.703 Log2-fold increased, respectively). According to qPCR results, the  
341 expressions of SLC1A4 and CRYZ in TRAMP group were only 0.15 and 0.62 fold of WT group.  
342 SLC1A4 was found to be associated with human hepatocellular carcinoma [54], and CRYZ was proven to  
343 be involved in BCL-2 overexpression in T-cell acute lymphocytic leukemia [55]. Although an association  
344 with prostate cancer was not found, our MeDIP-seq findings in the TRAMP model suggest that this  
345 association is possible.

346 Merged networks overlaid with IPA settings could even predict the direction of the relationship.  
347 When merging the two interesting networks HDAC2 and GSTP1 and overlaying the molecular activity  
348 predictor of IPA (Fig. 8), tumor protein 53 (TP53) was found to be located in the center of the novel  
349 network, indicating the potential important modulating function of TP53 on HDAC2 and GSTP1. TP53 is  
350 encoded by p53, a tumor suppressor gene located on chromosome 17p13, which is one of the most  
351 frequently mutated genes in various types of cancers [56-58]. TP53 acts as a transcription factor that  
352 mediates the response to many cellular stresses, most prominently, the DNA damage response [59]. TP53  
353 has also been proven to play a crucial role in prostate cancer development and progression [60-62].

354 The interactions between GSTP1, HDAC and TP53 have been studied in prostate disease models.  
355 In prostatectomy specimens of 30 benign prostatic hyperplasia patients, the increase in TP53 expression  
356 at the same site was accompanied by an increase in GSTP1 expression [63]. In the three prostate cancer

1  
2  
3  
4 357 cell lines DU-145, PC-3 and LNCaP, As<sub>2</sub>O<sub>3</sub> was found to increase TP53 expression only in LNCaP cells  
5  
6 358 (without GSTP1 expression) but not in DU-145 and PC-3 cells (both cells expressed GSTP1) [64]. In  
7  
8 359 LNCaP cells, the acetylation of human TP53 increased the binding of promoter fragments of the human  
9  
10 360 P21 gene that contained a p53 response element and of the human HDAC2 protein [65].  
11  
12

13 361 Although the relationships between TP53 and HDAC2 as well as GSTP1 in prostate cancer have  
14  
15 362 been elucidated, these relationships in the TRAMP model remain unknown. Our predicated interactions  
16  
17 363 among these proteins in TRAMP suggest the possibility that TP53 influences the methylation of GSTP1  
18  
19 364 and HDAC2, which is a potential direction of future research.  
20  
21

22 365  
23

24 366 **Conclusions**  
25  
26 367 To the best of our knowledge, this is the first MeDIP-seq study to analyze the DNA methylation  
27  
28 368 differences of prostate cancer by comparing TRAMP mice, an adenocarcinoma prostate cancer model,  
29  
30 369 with wild-type C57BL/6 mice. Cancer, especially adenocarcinoma, is the most commonly associated  
31  
32 370 disease. MSP and qPCR have been used to validate the findings of MeDIP-seq. Using this MeDIP-seq  
33  
34 371 and IPA analysis, comparisons between the TRAMP and control samples reveal profound differences in  
35  
36 372 gene methylation. The analysis of canonical pathways and networks has identified important biological  
37  
38 373 functions and molecular pathways that may mediate the development of adenocarcinoma prostate cancer.  
39  
40 374 CREB-, HDAC2-, GSTP1- and UBC-related pathways showed significantly altered methylation profiles  
41  
42 375 based on the canonical pathway and network analyses. Studies on epigenetics, such as DNA methylation,  
43  
44 376 suggest novel avenues and strategies for the further development of biomarkers targeted for treatment and  
45  
46 377 prevention approaches for prostate cancer.  
47  
48 378  
49  
50 379  
51  
52 380 **Conflict of interest statement**  
53  
54 381 The authors declare that there are no conflicts of interest.  
55  
56 382  
57  
58 383  
59  
60 384  
61  
62 385  
63  
64 386  
65

1  
2  
3  
4 383 **Authors' contributions**  
5

6 384 Wenji Li designed the experiments. Wenji Li, Ying Huang and Davit Sargsyan performed the  
7 experiments and acquired the data. All authors prepared the manuscript. All authors read and approved  
8 385 the final manuscript.  
9 386

10  
11 387  
12  
13 388 **Acknowledgments**  
14

15 389 The authors express sincere gratitude to all of the members of Dr. Tony Kong's laboratory for their  
16 helpful discussions. This work was supported in part by institutional funds and by R01-CA118947, R01-  
17 CA152826, and R01-CA200129 from the National Cancer Institute (NCI), R01-AT009152 from the  
18 391 National Center for Complementary and Integrative Health (NCCIH), and R01-AT007065 from NCCIH  
19 392 and the Office of Dietary Supplements (ODS).  
20 393  
21  
22  
23  
24  
25  
26  
27  
28  
29  
30  
31  
32  
33  
34  
35  
36  
37  
38  
39  
40  
41  
42  
43  
44  
45  
46  
47  
48  
49  
50  
51  
52  
53  
54  
55  
56  
57  
58  
59  
60  
61  
62  
63  
64  
65

4                   **References**

- 5  
6                   1. Ferlay J, Shin HR, Bray F, Forman D, Mathers C, Parkin DM: **Estimates of worldwide burden**  
7                   of **cancer in 2008: GLOBOCAN 2008.** *International journal of cancer* 2010, **127**:2893-2917.  
8  
9                   2. **United States Cancer Statistics: 1999–2011 Incidence and Mortality Web-based Report.**  
10                  [<http://apps.cancer.gov/uscs/>]  
11                  3. Barbieri CE, Bangma CH, Bjartell A, Catto JW, Culig Z, Gronberg H, Luo J, Visakorpi T, Rubin  
12                  MA: **The mutational landscape of prostate cancer.** *Eur Urol* 2013, **64**:567-576.  
13                  4. Cuzick J, Thorat MA, Andriole G, Brawley OW, Brown PH, Culig Z, Eeles RA, Ford LG,  
14                  Hamdy FC, Holmberg L, et al: **Prevention and early detection of prostate cancer.** *Lancet*  
15                  Oncol 2014, **15**:e484-e492.  
16                  5. Strand SH, Orntoft TF, Sorensen KD: **Prognostic DNA Methylation Markers for Prostate**  
17                  **Cancer.** *Int J Mol Sci* 2014, **15**:16544-16576.  
18  
19                  6. Matei DE, Nephew KP: **Epigenetic therapies for chemoresensitization of epithelial ovarian**  
20                  **cancer.** *Gynecol Oncol* 2010, **116**:195-201.  
21                  7. Jeong M, Goodell MA: **New answers to old questions from genome-wide maps of DNA**  
22                  **methylation in hematopoietic cells.** *Exp Hematol* 2014, **42**:609-617.  
23                  8. Ushijima T, Watanabe N, Okochi E, Kaneda A, Sugimura T, Miyamoto K: **Fidelity of the**  
24                  **methylation pattern and its variation in the genome.** *Genome Res* 2003, **13**:868-874.  
25                  9. Gama-Sosa MA, Slagel VA, Trewyn RW, Oxenhander R, Kuo KC, Gehrke CW, Ehrlich M: **The**  
26                  **5-methylcytosine content of DNA from human tumors.** *Nucleic Acids Res* 1983, **11**:6883-6894.  
27                  10. Brothman AR, Swanson G, Maxwell TM, Cui J, Murphy KJ, Herrick J, Speights VO, Isaac J,  
28                  Rohr LR: **Global hypomethylation is common in prostate cancer cells: a quantitative**  
29                  **predictor for clinical outcome?** *Cancer Genet Cytogenet* 2005, **156**:31-36.  
30                  11. Seifert HH, Schmiemann V, Mueller M, Kazimirek M, Onofre F, Neuhausen A, Florl AR,  
31                  Ackermann R, Boecking A, Schulz WA, Grote HJ: **In situ detection of global DNA**  
32                  **hypomethylation in exfoliative urine cytology of patients with suspected bladder cancer.** *Exp*  
33                  *Mol Pathol* 2007, **82**:292-297.  
34                  12. Issa JP: **CpG island methylator phenotype in cancer.** *Nat Rev Cancer* 2004, **4**:988-993.  
35                  13. Shaw RJ, Hall GL, Lowe D, Bowers NL, Liloglou T, Field JK, Woolgar JA, Risk JM: **CpG**  
36                  **island methylation phenotype (CIMP) in oral cancer: associated with a marked**  
37                  **inflammatory response and less aggressive tumour biology.** *Oral Oncol* 2007, **43**:878-886.  
38                  14. Nazemalhosseini Mojarrad E, Kuppen PJ, Aghdaei HA, Zali MR: **The CpG island methylator**  
39                  **phenotype (CIMP) in colorectal cancer.** *Gastroenterol Hepatol Bed Bench* 2013, **6**:120-128.  
40                  15. Berg M, Hagland HR, Soreide K: **Comparison of CpG island methylator phenotype (CIMP)**  
41                  **frequency in colon cancer using different probe- and gene-specific scoring alternatives on**  
42                  **recommended multi-gene panels.** *PLoS One* 2014, **9**:e86657.  
43                  16. Hurwitz AA, Foster BA, Allison JP, Greenberg NM, Kwon ED: **The TRAMP mouse as a model**  
44                  **for prostate cancer.** *Curr Protoc Immunol* 2001, Chapter 20:Unit 20 25.  
45                  17. Valkenburg KC, Williams BO: **Mouse models of prostate cancer.** *Prostate Cancer* 2011,  
46                  2011:**895238.**  
47                  18. Yu S, Khor TO, Cheung KL, Li W, Wu TY, Huang Y, Foster BA, Kan YW, Kong AN: **Nrf2**  
48                  **expression is regulated by epigenetic mechanisms in prostate cancer of TRAMP mice.** *PLoS*  
49                  *One* 2010, **5**:e8579.  
50                  19. McCabe MT, Low JA, Daignault S, Imperiale MJ, Wojno KJ, Day ML: **Inhibition of DNA**  
51                  **methyltransferase activity prevents tumorigenesis in a mouse model of prostate cancer.**  
52                  *Cancer Res* 2006, **66**:385-392.  
53                  20. Mavis CK, Morey Kinney SR, Foster BA, Karpf AR: **Expression level and DNA methylation**  
54                  **status of glutathione-S-transferase genes in normal murine prostate and TRAMP tumors.**  
55                  *Prostate* 2009, **69**:1312-1324.  
56  
57  
58  
59  
60  
61  
62  
63  
64  
65

- 1  
2  
3  
4 443 21. Pulukuri SM, Rao JS: **CpG island promoter methylation and silencing of 14-3-3sigma gene**  
5 444 **expression in LNCaP and Tramp-C1 prostate cancer cell lines is associated with methyl-**  
6 445 **CpG-binding protein MBD2.** *Oncogene* 2006, **25**:4559-4572.  
7 446 22. Chiam K, Ryan NK, Ricciardelli C, Day TK, Buchanan G, Ochnik AM, Murti K, Selth LA,  
8 447 Australian Prostate Cancer B, Butler LM, et al: **Characterization of the prostate cancer**  
9 448 **susceptibility gene KLF6 in human and mouse prostate cancers.** *Prostate* 2013, **73**:182-193.  
10 449 23. Morey Kinney SR, Zhang W, Pascual M, Greally JM, Gillard BM, Karasik E, Foster BA, Karpf  
11 450 AR: **Lack of evidence for green tea polyphenols as DNA methylation inhibitors in murine**  
12 451 **prostate.** *Cancer Prev Res (Phila)* 2009, **2**:1065-1075.  
13 452 24. Wu TY, Khor TO, Su ZY, Saw CL, Shu L, Cheung KL, Huang Y, Yu S, Kong AN: **Epigenetic**  
14 453 **modifications of Nrf2 by 3,3'-diindolylmethane in vitro in TRAMP C1 cell line and in vivo**  
15 454 **TRAMP prostate tumors.** *AAPS J* 2013, **15**:864-874.  
16 455 25. Khor TO, Yu S, Barve A, Hao X, Hong JL, Lin W, Foster B, Huang MT, Newmark HL, Kong  
17 456 AN: **Dietary feeding of dibenzoylmethane inhibits prostate cancer in transgenic**  
18 457 **adenocarcinoma of the mouse prostate model.** *Cancer Res* 2009, **69**:7096-7102.  
19 458 26. Trapnell C, Roberts A, Goff L, Pertea G, Kim D, Kelley DR, Pimentel H, Salzberg SL, Rinn JL,  
20 459 Pachter L: **Differential gene and transcript expression analysis of RNA-seq experiments with**  
21 460 **TopHat and Cufflinks.** *Nat Protoc* 2012, **7**:562-578.  
22 461 27. Zhu LJ, Gazin C, Lawson ND, Pages H, Lin SM, Lapointe DS, Green MR: **ChIPpeakAnno: a**  
23 462 **Bioconductor package to annotate ChIP-seq and ChIP-chip data.** *BMC Bioinformatics* 2010,  
24 463 **11**:237.  
25 464 28. Khor TO, Huang Y, Wu TY, Shu L, Lee J, Kong AN: **Pharmacodynamics of curcumin as DNA**  
26 465 **hypomethylation agent in restoring the expression of Nrf2 via promoter CpGs**  
27 466 **demethylation.** *Biochem Pharmacol* 2011, **82**:1073-1078.  
28 467 29. Wang D, Liang H, Mao X, Liu W, Li M, Qiu S: **Changes of transthyretin and clusterin after**  
29 468 **androgen ablation therapy and correlation with prostate cancer malignancy.** *Transl Oncol*  
30 469 2012, **5**:124-132.  
31 470 30. Jiang YZ, Manduchi E, Stoeckert CJ, Jr., Davies PF: **Arterial endothelial methylome:**  
32 471 **differential DNA methylation in athero-susceptible disturbed flow regions in vivo.** *BMC*  
33 472 *Genomics* 2015, **16**:506.  
34 473 31. Chiaverotti T, Couto SS, Donjacour A, Mao JH, Nagase H, Cardiff RD, Cunha GR, Balmain A:  
35 474 **Dissociation of epithelial and neuroendocrine carcinoma lineages in the transgenic**  
36 475 **adenocarcinoma of mouse prostate model of prostate cancer.** *Am J Pathol* 2008, **172**:236-246.  
37 476 32. Mayr B, Montminy M: **Transcriptional regulation by the phosphorylation-dependent factor**  
38 477 **CREB.** *Nat Rev Mol Cell Biol* 2001, **2**:599-609.  
39 478 33. Shaywitz AJ, Greenberg ME: **CREB: a stimulus-induced transcription factor activated by a**  
40 479 **diverse array of extracellular signals.** *Annu Rev Biochem* 1999, **68**:821-861.  
41 480 34. Sakamoto KM, Frank DA: **CREB in the pathophysiology of cancer: implications for targeting**  
42 481 **transcription factors for cancer therapy.** *Clin Cancer Res* 2009, **15**:2583-2587.  
43 482 35. Conkright MD, Montminy M: **CREB: the unindicted cancer co-conspirator.** *Trends Cell Biol*  
44 483 2005, **15**:457-459.  
45 484 36. Gibadulinova A, Tothova V, Pastorek J, Pastorekova S: **Transcriptional regulation and**  
46 485 **functional implication of S100P in cancer.** *Amino Acids* 2011, **41**:885-892.  
47 486 37. Tang H, Goldberg E: **Homo sapiens lactate dehydrogenase c (Ldhc) gene expression in**  
48 487 **cancer cells is regulated by transcription factor Sp1, CREB, and CpG island methylation.** *J*  
49 488 *Androl* 2009, **30**:157-167.  
50 489 38. Park MH, Lee HS, Lee CS, You ST, Kim DJ, Park BH, Kang MJ, Heo WD, Shin EY, Schwartz  
51 490 MA, Kim EG: **p21-Activated kinase 4 promotes prostate cancer progression through CREB.**  
52 491 *Oncogene* 2013, **32**:2475-2482.  
53 492 39. Xiao X, Li BX, Mitton B, Ikeda A, Sakamoto KM: **Targeting CREB for cancer therapy:**  
54 493 **friend or foe.** *Curr Cancer Drug Targets* 2010, **10**:384-391.  
55  
56  
57  
58  
59  
60  
61  
62  
63  
64  
65

- 1  
2  
3  
4 494 40. Bassett SA, Barnett MP: **The Role of Dietary Histone Deacetylases (HDACs) Inhibitors in**  
5 495 **Health and Disease.** *Nutrients* 2014, **6**:4273-4301.  
6 496 41. Glauben R, Batra A, Stroh T, Erben U, Fedke I, Lehr HA, Leoni F, Mascagni P, Dinarello CA,  
7 497 Zeitz M, Siegmund B: **Histone deacetylases: novel targets for prevention of colitis-associated**  
8 498 **cancer in mice.** *Gut* 2008, **57**:613-622.  
9 499 42. Giannini G, Cabri W, Fattorusso C, Rodriguez M: **Histone deacetylase inhibitors in the**  
10 500 **treatment of cancer: overview and perspectives.** *Future Med Chem* 2012, **4**:1439-1460.  
11 501 43. Kim HJ, Bae SC: **Histone deacetylase inhibitors: molecular mechanisms of action and**  
12 502 **clinical trials as anti-cancer drugs.** *Am J Transl Res* 2011, **3**:166-179.  
13 503 44. Qian DZ, Wei YF, Wang X, Kato Y, Cheng L, Pili R: **Antitumor activity of the histone**  
14 504 **deacetylase inhibitor MS-275 in prostate cancer models.** *Prostate* 2007, **67**:1182-1193.  
15 505 45. Sargeant AM, Rengel RC, Kulp SK, Klein RD, Clinton SK, Wang YC, Chen CS: **OSU-HDAC42,**  
16 506 **a histone deacetylase inhibitor, blocks prostate tumor progression in the transgenic**  
17 507 **adenocarcinoma of the mouse prostate model.** *Cancer Res* 2008, **68**:3999-4009.  
18 508 46. He GH, Lin JJ, Cai WK, Xu WM, Yu ZP, Yin SJ, Zhao CH, Xu GL: **Associations of**  
19 509 **polymorphisms in histidine decarboxylase, histamine N-methyltransferase and histamine**  
20 510 **receptor H3 genes with breast cancer.** *PLoS One* 2014, **9**:e97728.  
21 511 47. Roh T, Kwak MY, Kwak EH, Kim DH, Han EY, Bae JY, Bang du Y, Lim DS, Ahn IY, Jang DE,  
22 512 et al: **Chemopreventive mechanisms of methionine on inhibition of benzo(a)pyrene-DNA**  
23 513 **adducts formation in human hepatocellular carcinoma HepG2 cells.** *Toxicol Lett* 2012,  
24 514 **208**:232-238.  
25 515 48. Nelson WG, De Marzo AM, DeWeese TL, Isaacs WB: **The role of inflammation in the**  
26 516 **pathogenesis of prostate cancer.** *J Urol* 2004, **172**:S6-11; discussion S11-12.  
27 517 49. Lin X, Tascilar M, Lee WH, Vles WJ, Lee BH, Veeraswamy R, Asgari K, Freije D, van Rees B,  
28 518 Gage WR, et al: **GSTP1 CpG island hypermethylation is responsible for the absence of**  
29 519 **GSTP1 expression in human prostate cancer cells.** *Am J Pathol* 2001, **159**:1815-1826.  
30 520 50. Nelson CP, Kidd LC, Sauvageot J, Isaacs WB, De Marzo AM, Groopman JD, Nelson WG,  
31 521 Kensler TW: **Protection against 2-hydroxyamino-1-methyl-6-phenylimidazo[4,5-b]pyridine**  
32 522 **cytotoxicity and DNA adduct formation in human prostate by glutathione S-transferase P1.**  
33 523 *Cancer Res* 2001, **61**:103-109.  
34 524 51. Maldonado L, Braith M, Loyo M, Sullenberger L, Wang K, Peskoe SB, Rosenbaum E, Howard R,  
35 525 Toubaji A, Albadine R, et al: **GSTP1 promoter methylation is associated with recurrence in**  
36 526 **early stage prostate cancer.** *J Urol* 2014, **192**:1542-1548.  
37 527 52. Bryzgunova OE, Morozkin ES, Yarmoschuk SV, Vlassov VV, Laktionov PP: **Methylation-**  
38 528 **specific sequencing of GSTP1 gene promoter in circulating/extracellular DNA from blood**  
39 529 **and urine of healthy donors and prostate cancer patients.** *Ann NY Acad Sci* 2008, **1137**:222-  
40 530 225.  
41 531 53. Dong H, Zhang H, Liang J, Yan H, Chen Y, Shen Y, Kong Y, Wang S, Zhao G, Jin W: **Digital**  
42 532 **karyotyping reveals probable target genes at 7q21.3 locus in hepatocellular carcinoma.**  
43 533 *BMC Med Genomics* 2011, **4**:60.  
44 534 54. Marshall A, Lukk M, Kutter C, Davies S, Alexander G, Odom DT: **Global gene expression**  
45 535 **profiling reveals SPINK1 as a potential hepatocellular carcinoma marker.** *PloS one* 2013,  
46 536 **8**:e59459.  
47 537 55. Lapucci A, Lulli M, Amedei A, Papucci L, Witort E, Di Gesualdo F, Bertolini F, Brewer G,  
48 538 Nicolin A, Bevilacqua A, et al: **zeta-Crystallin is a bcl-2 mRNA binding protein involved in**  
49 539 **bcl-2 overexpression in T-cell acute lymphocytic leukemia.** *FASEB J* 2010, **24**:1852-1865.  
50 540 56. Wang X, Zhang X, He P, Fang Y: **Sensitive detection of p53 tumor suppressor gene using an**  
51 541 **enzyme-based solid-state electrochemiluminescence sensing platform.** *Biosens Bioelectron*  
52 542 **2011, 26**:3608-3613.  
53 543 57. Parkinson EK: **Senescence as a modulator of oral squamous cell carcinoma development.**  
54 544 *Oral Oncol* 2010, **46**:840-853.  
55  
56  
57  
58  
59  
60  
61  
62  
63  
64  
65

- Hickman JA, Potten CS, Merritt AJ, Fisher TC: **Apoptosis and cancer chemotherapy.** *Philos Trans R Soc Lond B Biol Sci* 1994, **345**:319-325.
- Rokavec M, Li H, Jiang L, Hermeking H: **The p53/microRNA connection in gastrointestinal cancer.** *Clin Exp Gastroenterol* 2014, **7**:395-413.
- Thomas P, Pang Y, Dong J, Berg AH: **Identification and Characterization of Membrane Androgen Receptors in the ZIP9 Zinc Transporter Subfamily: II. Role of Human ZIP9 in Testosterone-Induced Prostate and Breast Cancer Cell Apoptosis.** *Endocrinology* 2014, **155**:4250-4265.
- Lin VC, Huang CY, Lee YC, Yu CC, Chang TY, Lu TL, Huang SP, Bao BY: **Genetic variations in TP53 binding sites are predictors of clinical outcomes in prostate cancer patients.** *Arch Toxicol* 2014, **88**:901-911.
- Antonarakis ES, Keizman D, Zhang Z, Gurel B, Lotan TL, Hicks JL, Fedor HL, Carducci MA, De Marzo AM, Eisenberger MA: **An immunohistochemical signature comprising PTEN, MYC, and Ki67 predicts progression in prostate cancer patients receiving adjuvant docetaxel after prostatectomy.** *Cancer* 2012, **118**:6063-6071.
- Wang W, Bergh A, Damber JE: **Increased p53 immunoreactivity in proliferative inflammatory atrophy of prostate is related to focal acute inflammation.** *APMIS* 2009, **117**:185-195.
- Lu M, Xia L, Luo D, Waxman S, Jing Y: **Dual effects of glutathione-S-transferase pi on As2O3 action in prostate cancer cells: enhancement of growth inhibition and inhibition of apoptosis.** *Oncogene* 2004, **23**:3945-3952.
- Roy S, Tenniswood M: **Site-specific acetylation of p53 directs selective transcription complex assembly.** *J Biol Chem* 2007, **282**:4765-4771.

1  
2  
3  
4 570 Table Legends  
5  
6 571  
7  
8 572 Table 1 Primer sequences used in MSP  
9  
10 573  
11  
12 574 Table 2 Primer sequences used in qPCR  
13  
14  
15 575  
16  
17 576 Table 3 Top 50 annotated genes with increased methylation, ranked by log<sub>2</sub>-fold change  
18  
19 577  
20  
21 578 Table 4 Top 50 annotated genes with decreased methylation, ranked by log<sub>2</sub>-fold change  
22  
23  
24 579  
25  
26 580 Table 5 Top 10 altered canonical pathways, sorted by -log<sub>10</sub> (P) value via IPA  
27  
28 581  
29  
30 582 Table 6 Top networks analyzed by IPA  
31  
32 583  
33  
34 584 Table 7 Altered methylation genes mapped to the neuropathic pain signaling pathway by IPA  
35  
36  
37 585  
38  
39 586  
40  
41 587  
42  
43 588  
44  
45 589  
46  
47 590  
48  
49  
50 591  
51  
52 592  
53  
54 593  
55  
56 594  
57  
58 595  
59  
60  
61  
62  
63  
64  
65

- 1  
2  
3  
4 596 Figure Legends  
5  
6 597 Fig. 1 Total mapping reads in the control and TRAMP mice (A) and the total number of significantly  
7 (log<sub>2</sub>-fold change  $\geq 2$ ) increased and decreased methylated genes in the TRAMP mice compared with the  
8 control mice (B)  
9  
10  
11 600 Fig. 2 Heat-map of Top 100 decreased or increased (Log<sub>2</sub>-fold Change) methylated genes comparing  
12 with TRAMP to WT in different regions by MeDIP analysis, ranked by alphabetic.  
13  
14  
15 602 Fig 3 Medip-Seq Validation by methylation-specific PCR (MSP). Representative electrophoretogram is  
16 presented in the top panel. M-MSP: methylated reaction of MSP, U-MSP: unmethylated reaction of MSP.  
17 The relative intensity of the methylated and unmethylated band was measured by ImageJ and presented in  
18 the bottom panel. All of the data are presented as the mean  $\pm$  SD. \* $p < 0.05$  versus the control WT group.  
19  
20  
21 606 Fig. 4. Comparison of mRNA expression of CRYZ, DYNC1I1, HNMT, SLC1A4 and TTR among WT  
22 and TRAMP mice prostate samples. Total mRNA was isolated and analyzed using quantitative real-time  
23 PCR. The data are presented as the mean  $\pm$  SD of three independent experiments. \* $p < 0.05$  versus the  
24 control WT group.  
25  
26  
27 610 Fig. 5. Top 5 associated disease categories (A) and top 5 cancer subtypes (B) analyzed by IPA  
28  
29  
30 611 Fig. 6 Genes mapped to the canonical neuropathic pain signaling pathway by IPA. Red, increased  
31 methylation; green, decreased methylation (for interpretation of the references to color in the figure  
32 legend, please refer to the online version of this article)  
33  
34 614  
35  
36 615 Fig. 7 HDAC2 network (Score=38) (A), GSTP1 network (Score=16) (B), and UBC network (Score=16)  
37 (C), as determined by IPA. Red, increased methylation; green, decreased methylation (for interpretation  
38 of the references to color in the figure legend, please refer to the online version of this article)  
39  
40  
41 618  
42  
43 619 Fig. 8 Merged network of the HDAC2 and GSTP1 networks, as determined by IPA. Red, increased  
44 methylation; green, decreased methylation (for interpretation of the references to color in the figure  
45 legend, please refer to the online version of this article)  
46  
47  
48  
49  
50  
51  
52  
53  
54  
55  
56  
57  
58  
59  
60  
61  
62  
63  
64  
65

Table 1 Primer sequences used in MSP

Gene name	Primer name	Primer sequence	Band size (bp)
<b>Dync1i1</b>	Dync1i1-MF*	TATGAAGAAAAATATAAGATAACGG	232
	Dync1i1-MR*	ACGAACATTCACATTCGAA	
	Dync1i1-UF*	TTTATGAAGAAAAATATAAGATAATGG	235
	Dync1i1-UR*	CACAAACATTCACATTCAAA	
<b>Slc1a4</b>	Slc1a4-MF	ATAAATTATTTTTTATGTTACGG	216
	Slc1a4-MR	TTAATAATACATACCTATAATCCGAC	
	Slc1a4-UF	ATAAATTATTTTTTATGTTATGG	216
	Slc1a4-UR	TTAATAATACATACCTATAATCCAAC	
<b>Xrcc6bp1</b>	Xrcc6bp1-MF	GTAAATGTGAGAGTTAGAATAGTATAGGAC	110
	Xrcc6bp1-MR	AATTAATACAATATTCGATACCGAT	
	Xrcc6bp1-UF	GTAAATGTGAGAGTTAGAATAGTATAGGAT	110
	Xrcc6bp1-UR	AATTAATACAATATTCAAATACCAAT	
<b>TTR</b>	TTR-MF	GGAATTAAAGATAACGGTTATATCGA	106
	TTR-MR	AACACTCTTCGAACATACTCGAC	
	TTR-UF	AGGAATTAAAGATATGGTTATATTGA	108
	TTR-UR	AAACACTCTTCAAACATACTCAAC	

\*:-MF: forward primer sequence for the methylated reactions; -MR: reverse primer sequence for the unmethylated reactions;-UF: forward primer sequence for the unmethylated reactions; -UR: reverse primer sequence for the unmethylated reactions. Primer sequences are started from 5' (left) to 3' (right).

Table 2 Primer sequences used in qPCR

<b>Gene name</b>	<b>Primer name</b>	<b>Primer sequence</b>
<b>HNMT</b>	sense	5' -GCTGCCAGTGCTAAAATTCTC -3'
	antisense	5' -CAGGTCATCCAGTATCTGCG -3'
<b>DYNC1I1</b>	sense	5' -GTGTACGATGTCATGTGGTCC-3'
	antisense	5' -AACTCGGTTAG GGCAGATG-3'
<b>SLC1A4</b>	sense	5' -CCTCACATTGCCATCATCTT G-3'
	antisense	5' -CATCCCCTCCACATTCAACC-3'
<b>CRYZ</b>	sense	5' -GCAGCCGATGACACTATCTAC-3'
	antisense	5' -GCCCATGAACCAAAACG -3'
<b>TTR</b>	sense	5' -AATCGTACTGGAAGACACTTGG-3'
	antisense	5' -TGGTGCTGTAGGAGTATGGG -3'
<b>β-Actin</b>	sense	5' -CGTTCAATACCCCAGCCATG-3'
	antisense	5' -ACCCCGTCACCAGAGTCC-3'

Table 3 Top 50 annotated genes with increased methylation, ranked by log<sub>2</sub>-fold change

Rank	Symbol	Gene Name	Log <sub>2</sub> -fold Change	Location	Type(s)	Methylation Region
(TRAMP/WT)						
1	FGD4	FYVE, RhoGEF and PH domain containing 4	4.993	Cytoplasm	other	promoter
2	MED13L	mediator complex subunit 13-like	4.993	Nucleus	other	downstream
3	DYNC1I1	dynein, cytoplasmic 1, intermediate chain 1	4.926	Cytoplasm	other	body
4	XK	X-linked Kx blood group	4.781	Plasma Membrane	transporter	body
5	EAPP	E2F-associated phosphoprotein	4.703	Cytoplasm	other	body
6	TGFA	transforming growth factor, alpha	4.534	Extracellular Space	growth factor	promoter
7	BTG1	B-cell translocation gene 1, anti-proliferative	4.440	Nucleus	transcription regulator	promoter
8	BARD1	BRCA1 associated RING domain 1	4.341	Nucleus	transcription regulator	promoter
9	GJA1	gap junction protein, alpha 1, 43 kDa	4.341	Plasma Membrane	transporter	promoter
10	Zfp640	zinc finger protein 640	4.234	Other	other	downstream
11	S100A5	S100 calcium-binding protein A5	4.119	Nucleus	other	promoter
12	SOX17	SRY (sex-determining region	4.119	Nucleus	transcription	downstream

		Y)-box 17			regulator	
13	PDGFRL	platelet-derived growth factor receptor-like	3.993	Plasma Membrane	kinase	body
14	ZKSCAN2	zinc finger with KRAB and SCAN domains 2	3.993	Nucleus	transcription regulator	promoter
15	DMXL2	Dmx-like 2	3.926	Cytoplasm	other	body
16	LEPR	leptin receptor	3.926	Plasma Membrane	transmembrane receptor	body
17	AOAH	acyloxyacyl hydrolase (neutrophil)	3.855	Extracellular Space	enzyme	promoter
18	Apol7e	apolipoprotein L 7e	3.855	Other	other	body
19	CACNG6	calcium channel, voltage-dependent, gamma subunit 6	3.855	Plasma Membrane	ion channel	promoter
20	CHCHD3	coiled-coil-helix-coiled-coil-helix domain containing 3	3.855	Cytoplasm	other	body
21	FAM174B	family with sequence similarity 174, member B	3.855	Other	other	body
22	GALNT13	polypeptide N-acetylgalactosaminyltransferase	3.855	Cytoplasm	enzyme	body
23	GPR37	G protein-coupled receptor 37 (endothelin receptor type B-like)	3.855	Plasma Membrane	G-protein coupled receptor	downstream
24	Mup1	major urinary protein 1	3.855	Extracellular Space	other	downstream

<b>25</b>	NGF	nerve growth factor (beta polypeptide)	3.855	Extracellular Space	growth factor	downstream
<b>26</b>	OLFM3	olfactomedin 3	3.855	Cytoplasm	other	body
<b>27</b>	PCBP3	poly(rC)-binding protein 3	3.855	Nucleus	other	body
<b>28</b>	RBMS3	RNA-binding motif, single-stranded-interacting protein 3	3.855	Other	other	body
<b>29</b>	TMX1	thioredoxin-related transmembrane protein 1	3.855	Cytoplasm	enzyme	downstream
<b>30</b>	ZNF14	zinc finger protein 14	3.855	Nucleus	transcription regulator	body
<b>31</b>	SLC1A4	solute carrier family 1 (glutamate/neutral amino acid transporter), member 4	3.807	Plasma Membrane	transporter	body
<b>32</b>	ZFAND3	zinc finger, AN1-type domain 3	3.717	Other	other	body
<b>33</b>	C1orf162	chromosome 1 open reading frame 162	3.703	Other	transporter	promoter
<b>34</b>	C9orf131	chromosome 9 open reading frame 131	3.703	Other	other	body
<b>35</b>	CRYZ	crystallin, zeta (quinone reductase)	3.703	Cytoplasm	enzyme	body
<b>36</b>	CYP2A6	cytochrome P450, family 2, subfamily A, polypeptide 6	3.703	Cytoplasm	enzyme	body
<b>37</b>	CYP51A1	cytochrome P450, family 51, subfamily A, polypeptide 1	3.703	Cytoplasm	enzyme	downstream
<b>38</b>	DSPP	dentin sialophosphoprotein	3.703	Extracellular	other	promoter

Space						
<b>39</b>	GALNT3	polypeptide N-acetylgalactosaminyltransferase 3	3.703	Cytoplasm	enzyme	downstream
<b>40</b>	Gm4836	predicted gene 4836	3.703	Nucleus	other	downstream
<b>41</b>	GRIP1	glutamate receptor-interacting protein 1	3.703	Plasma Membrane	transcription regulator	promoter
<b>42</b>	GUCY1A2	guanylate cyclase 1, soluble, alpha 2	3.703	Cytoplasm	enzyme	body
<b>43</b>	HNMT	histamine N-methyltransferase	3.703	Cytoplasm	enzyme	body
<b>44</b>	LRRC8B	Leucine-rich repeat containing 8 family, member B	3.703	Other	other	body
<b>45</b>	MEF2A	myocyte enhancer factor 2A	3.703	Nucleus	transcription regulator	body
<b>46</b>	NRG3	neuregulin 3	3.703	Extracellular Space	growth factor	promoter
<b>47</b>	PCDH17	protocadherin 17	3.703	Other	other	promoter
<b>48</b>	PDP2	pyruvate dehydrogenase phosphatase catalytic subunit 2	3.703	Cytoplasm	phosphatase	promoter
<b>49</b>	SH2D4B	SH2 domain containing 4B	3.703	Other	other	body
<b>50</b>	Smok2b	sperm motility kinase 2B	3.703	Other	kinase	body

Table 4 Top 50 annotated genes with decreased methylation, ranked by log<sub>2</sub>-fold change

Ran k	Symbol	Gene Name	Log <sub>2</sub> fold Change	Location	Type(s)	Methylatio n region
			(TRAMP/W T)			
<b>1</b>	Rrbp1	Ribosome-binding protein 1	-5.824	Cytoplasm	transporter	body
<b>2</b>	CISD2	CDGSH iron sulfur domain 2	-4.373	Cytoplasm	other	downstream
<b>3</b>	NR4A1	nuclear receptor subfamily 4, group A, member 1	-4.324	Nucleus	ligand- dependent nuclear receptor	body
<b>4</b>	LCMT1	leucine carboxyl methyltransferase 1	-4.051	Cytoplasm	enzyme	body
<b>5</b>	XRCC6BP 1	XRCC6 binding protein 1	-3.990	Other	kinase	downstream
<b>6</b>	TTR	transthyretin	-3.926	Extracellular Space	transporter	promoter
<b>7</b>	ZNF536	zinc finger protein 536	-3.859	Other	other	downstream
<b>8</b>	FARP1	FERM, RhoGEF (ARHGEF) and pleckstrin domain protein 1	-3.788	Plasma Membrane	other	body

---

(chondrocyte-

derived)

<b>9</b>	TNRC18	trinucleotide repeat containing 18	-3.788	Other	other	body
<b>10</b>	FOXL1	forkhead box L1	-3.714	Nucleus	transcription	downstream regulator
<b>11</b>	ZMAT4	zinc finger, matrin- type 4	-3.714	Nucleus	other	promoter
<b>12</b>	ABCC2	ATP-binding cassette, sub-family C (CFTR/MRP), member 2	-3.636	Plasma Membrane	transporter	body
<b>13</b>	AMFR	autocrine motility factor receptor, E3 ubiquitin protein ligase	-3.636	Plasma Membrane	transmembran e receptor	downstream
<b>14</b>	ARSK	arylsulfatase family, member K	-3.636	Extracellular Space	enzyme	body
<b>15</b>	GRM3	glutamate receptor, metabotropic 3	-3.636	Plasma Membrane	G-protein coupled receptor	promoter
<b>16</b>	HTR1F	5- hydroxytryptamine (serotonin) receptor 1F, G protein-	-3.636	Plasma Membrane	G-protein coupled receptor	body

---

---

		coupled				
<b>17</b>	CC2D2A	coiled-coil and C2 domain containing 2A	-3.554	Other	other	promoter
<b>18</b>	CSMD1	CUB and Sushi multiple domains 1	-3.554	Plasma	other	body
<b>19</b>	HIBCH	3-hydroxyisobutyryl-CoA hydrolase	-3.554	Cytoplasm	enzyme	body
<b>20</b>	NMT2	N-myristoyltransferase 2	-3.554	Cytoplasm	enzyme	promoter
<b>21</b>	PCDH20	protocadherin 20	-3.554	Other	other	promoter
<b>22</b>	PDCD1	programmed cell death 1	-3.554	Plasma	phosphatase	promoter
<b>23</b>	QRFP	pyroglutamylated RFamide peptide	-3.554	Extracellular Space	other	downstream
<b>24</b>	REG3G	regenerating islet-derived 3 gamma	-3.554	Extracellular Space	other	downstream
<b>25</b>	TLR4	toll-like receptor 4	-3.554	Plasma	transmembrane receptor	downstream
<b>26</b>	TNRC6B	trinucleotide repeat containing 6B	-3.554	Other	other	body
<b>27</b>	CCR3	chemokine (C-C motif) receptor 3	-3.466	Plasma	G-protein coupled	promoter

---

receptor						
<b>28</b>	Cngb1	cyclic nucleotide gated channel beta 1	-3.466	Other	other	body
<b>29</b>	CNTNAP5	contactin associated protein-like 5	-3.466	Other	other	body
<b>30</b>	Cox7c	cytochrome c oxidase subunit VIIc	-3.466	Cytoplasm	other	promoter
<b>31</b>	EIF4EBP1	eukaryotic translation initiation factor 4E binding protein 1	-3.466	Cytoplasm	translation regulator	downstream
<b>32</b>	FGF10	fibroblast growth factor 10	-3.466	Extracellular Space	growth factor	downstream
<b>33</b>	GNAI1	guanine nucleotide-binding protein (G protein), alpha inhibiting activity polypeptide 1	-3.466	Plasma Membrane	enzyme	promoter
<b>34</b>	Ins1	insulin I	-3.466	Extracellular Space	other	promoter
<b>35</b>	ITGA8	integrin, alpha 8	-3.466	Plasma Membrane	other	body
<b>36</b>	JAG1	jagged 1	-3.466	Extracellular Space	growth factor	promoter

<b>37</b>	Pcdh10	protocadherin 10	-3.466	Other	other	promoter
<b>38</b>	PPP1R17	protein phosphatase subunit 17, regulatory	-3.466	Cytoplasm	other	downstream
<b>39</b>	Serbp1	Serpine1 mRNA-binding protein 1	-3.466	Cytoplasm	other	promoter
<b>40</b>	Wasl	Wiskott-Aldrich syndrome-like (human)	-3.466	Cytoplasm	other	promoter
<b>41</b>	ABAT	4-aminobutyrate aminotransferase	-3.373	Cytoplasm	enzyme	body
<b>42</b>	ANKMY2	ankyrin repeat and MYND domain containing 2	-3.373	Plasma Membrane	other	downstream
<b>43</b>	Card11	caspase recruitment domain family, member 11	-3.373	Other	other	body
<b>44</b>	CDK5R1	cyclin-dependent kinase 5, regulatory subunit 1 (p35)	-3.373	Nucleus	kinase	downstream
<b>45</b>	DACH1	dachshund family transcription factor 1	-3.373	Nucleus	transcription regulator	downstream
<b>46</b>	FGGY	FGGY carbohydrate kinase domain	-3.373	Other	other	body

---

		containing					
47	GADD45G	growth arrest and DNA-damage- inducible, gamma	-3.373	Nucleus	other		downstream
48	GLRB	glycine receptor, beta	-3.373	Plasma	ion channel	body	
49	LRRTM1	Leucine-rich repeat transmembrane neuronal 1	-3.373	Plasma	other		downstream
50	NEDD4L	neural precursor cell expressed, developmentally down-regulated 4- like, E3 ubiquitin protein ligase	-3.373	Cytoplasm	enzyme	body	

---

Table 5 Top 10 altered canonical pathways, sorted by  $-\log_{10}(P)$  value via IPA

Pathways	$-\log_{10}(p\text{-value})$	Involved Molecules
<b>Neuropathic Pain</b>	3.01	TACR1, GRM7, KCNN3, CAMK1D, MAPK1, GPR37, BDNF,
<b>Signaling In Dorsal Horn Neurons</b>		GRM3, GRIA1, CREB1, TAC1, GRIN3A
<b>Cardiomyocyte Differentiation via BMP Receptors</b>	3.01	NKX2-5, MAP3K7, SMAD6, MEF2C, BMP10
<b>cAMP-mediated Signaling</b>	2.75	ENPP6, ADCY2, RGS18, MAPK1, CAMK1D, PTGER3, GRM3, DUSP6, GNAI1, CHRM3, Cngb1, GRM7, FSHR, RGS10, CREB1, HTR1F, DRD3, PTGER4, PPP3CA
<b>Estrogen Biosynthesis</b>	2.64	CYP4F8, CYP3A5, HSD17B7, CYP2C9, CYP2A6 (includes others), CYP51A1, CYP2C8
<b>PXR/RXR Activation</b>	2.63	CYP3A5, ABCC2, INS, CYP2C9, CYP2A6 (includes others), INSR, PAPSS2, Ins1, CYP2C8
<b>Wnt/β-catenin Signaling</b>	2.43	CDKN2A, GJA1, WNT3, APPL2, APC, SOX17, SOX2, FZD8, PPP2R1A, WNT7A, RARB, TLE4, MAP3K7, NR5A2, GSK3B
<b>BMP Signaling Pathway</b>	2.43	MAP2K4, NKX2-5, MAPK1, BMP8A, CREB1, MAP3K7, SMAD6, GREM1, BMP10
<b>Factors Promoting Cardiogenesis in Vertebrates</b>	2.41	FZD8, SMAD2, NKX2-5, WNT3, BMP8A, MAP3K7, MEF2C, GSK3B, BMP10, APC
<b>Glutamate</b>	2.40	GRM7, SLC1A4, GRM3, GRIA1, SLC38A1, GRIP1, GRIK2,

<b>Receptor Signaling</b>	GRIN3A
<b>Human Embryonic Stem Cell</b>	2.39 SOX2, FZD8, SMAD2, WNT7A, WNT3, BDNF, BMP8A, SMAD6, GSK3B, NGF, APC, INHBA, BMP10
<b>Pluripotency</b>	
<b>LPS/IL-1 Mediated</b>	2.37 MAP2K4, GAL3ST2, ABCC2, CYP2C9, APOC2, NDST4, PAPSS2, IL1R2, TLR4, UST, CYP3A5, Sult1c2 (includes others), MAP3K7, NR5A2, CYP2A6 (includes others), GSTP1, MAOA, CYP2C8
<b>Inhibition of RXR Function</b>	

Table 6 Top networks analyzed by IPA

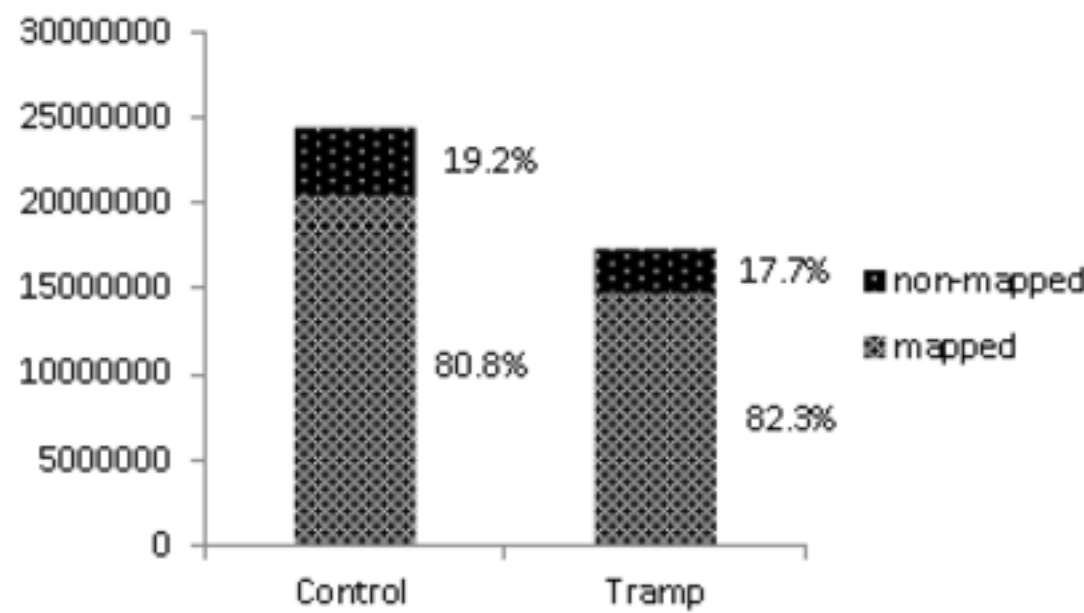
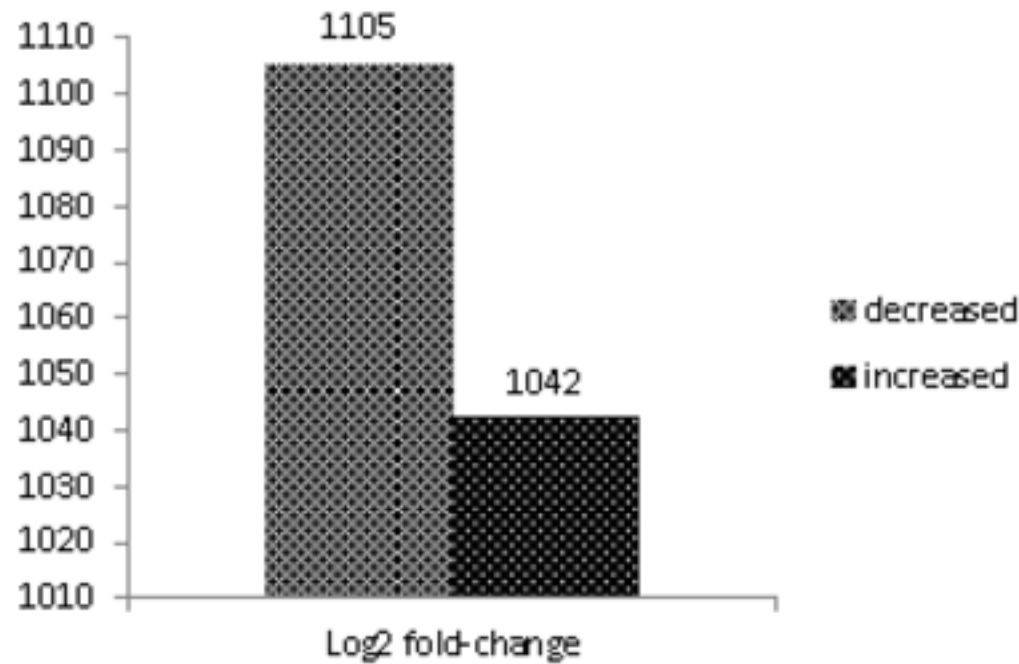
<b>Rank</b>	<b>Top Diseases and Functions</b>	<b>Score</b>
<b>1</b>	Tissue Morphology, Embryonic Development, Organ Development	38
<b>2</b>	Cell-To-Cell Signaling and Interaction, Cell Signaling, Cellular Function and Maintenance	38
<b>3</b>	Cell Death and Survival, Cancer, Cell Morphology	37
<b>4</b>	Cancer, Gastrointestinal Disease, Cell Death and Survival	35
<b>5</b>	Cancer, Carbohydrate Metabolism, Small Molecule Biochemistry	33
<b>6</b>	Cancer, Cell Death and Survival, Cellular Response to Therapeutics	33
<b>7</b>	Lymphoid Tissue Structure and Development, Organ Morphology, Organismal Development	30
<b>8</b>	Cancer, Gastrointestinal Disease, Post-Translational Modification	29
<b>9</b>	Cancer, Dermatological Diseases and Conditions, Gastrointestinal Disease	29
<b>10</b>	Cell Morphology, Digestive System Development and Function, Nervous System Development and Function	28
<b>11</b>	Cancer, Gastrointestinal Disease, Cell Death and Survival	26
<b>12</b>	Cancer, Drug Metabolism, Energy Production	26
<b>13</b>	Cell-To-Cell Signaling and Interaction, Nervous System Development and Function, Cellular Development	26
<b>14</b>	Cellular Movement, Cellular Development, Skeletal and Muscular System Development and Function	24
<b>15</b>	Cell Death and Survival, Cancer, Cellular Development	24
<b>16</b>	Hereditary Disorder, Inflammatory Response, Metabolic Disease	22

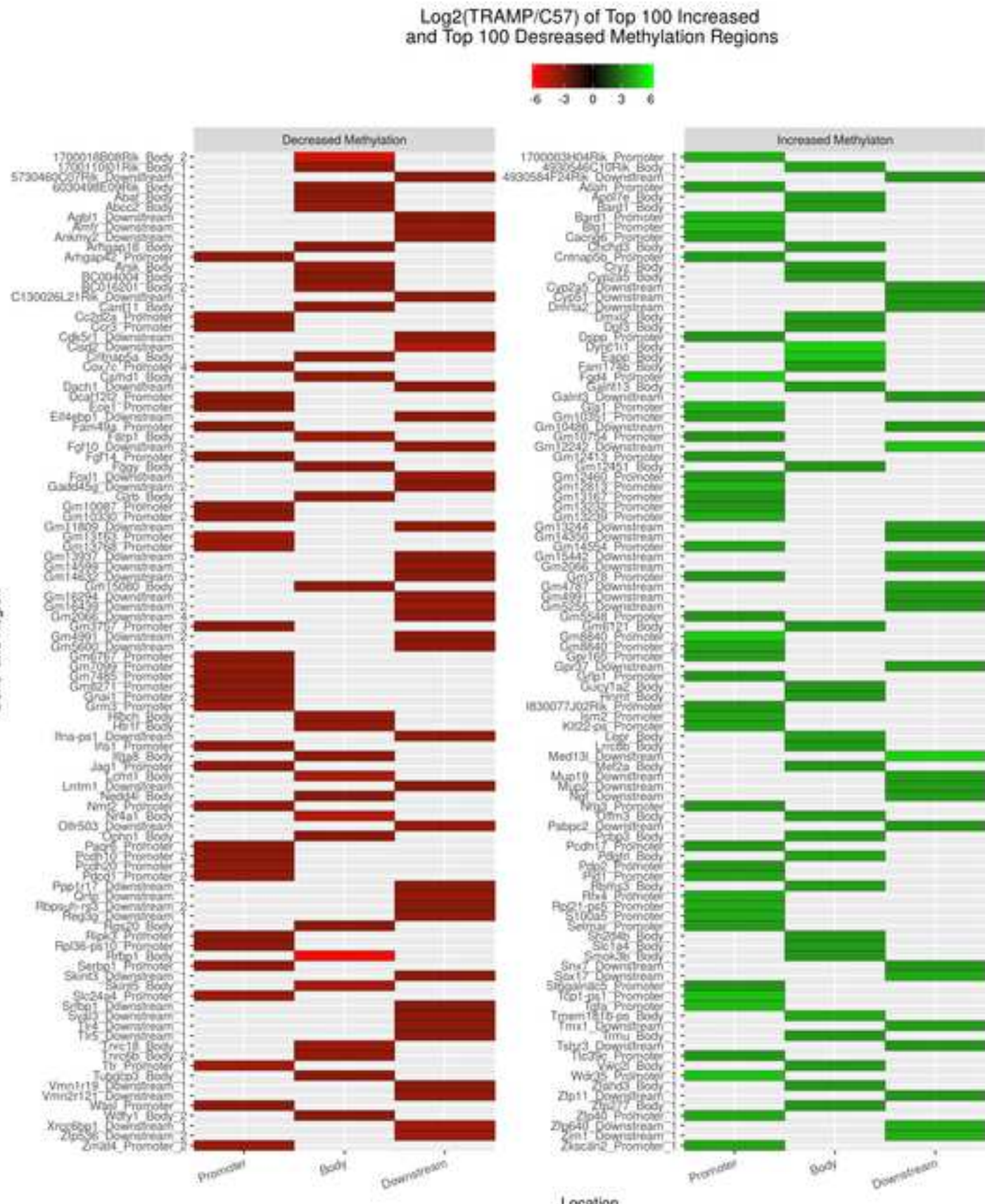
<b>17</b>	Cell Morphology, Nervous System Development and Function, Tissue Morphology	21
<b>18</b>	Cancer, Organismal Injury and Abnormalities, Reproductive System Disease	21
<b>19</b>	Cellular Compromise, Cancer, Cardiovascular Disease	19
<b>20</b>	Cell-To-Cell Signaling and Interaction, Tissue Development, Hematological System Development and Function	17
<b>21</b>	Cancer, Organismal Survival, Organismal Injury and Abnormalities	16
<b>22</b>	Cellular Assembly and Organization, Cellular Function and Maintenance, Embryonic Development	16
<b>23</b>	Cancer, Organismal Injury and Abnormalities, Reproductive System Disease	16
<b>24</b>	Cell Cycle, Cellular Movement, Cancer	16
<b>25</b>	Cancer, Developmental Disorder, Hereditary Disorder	16

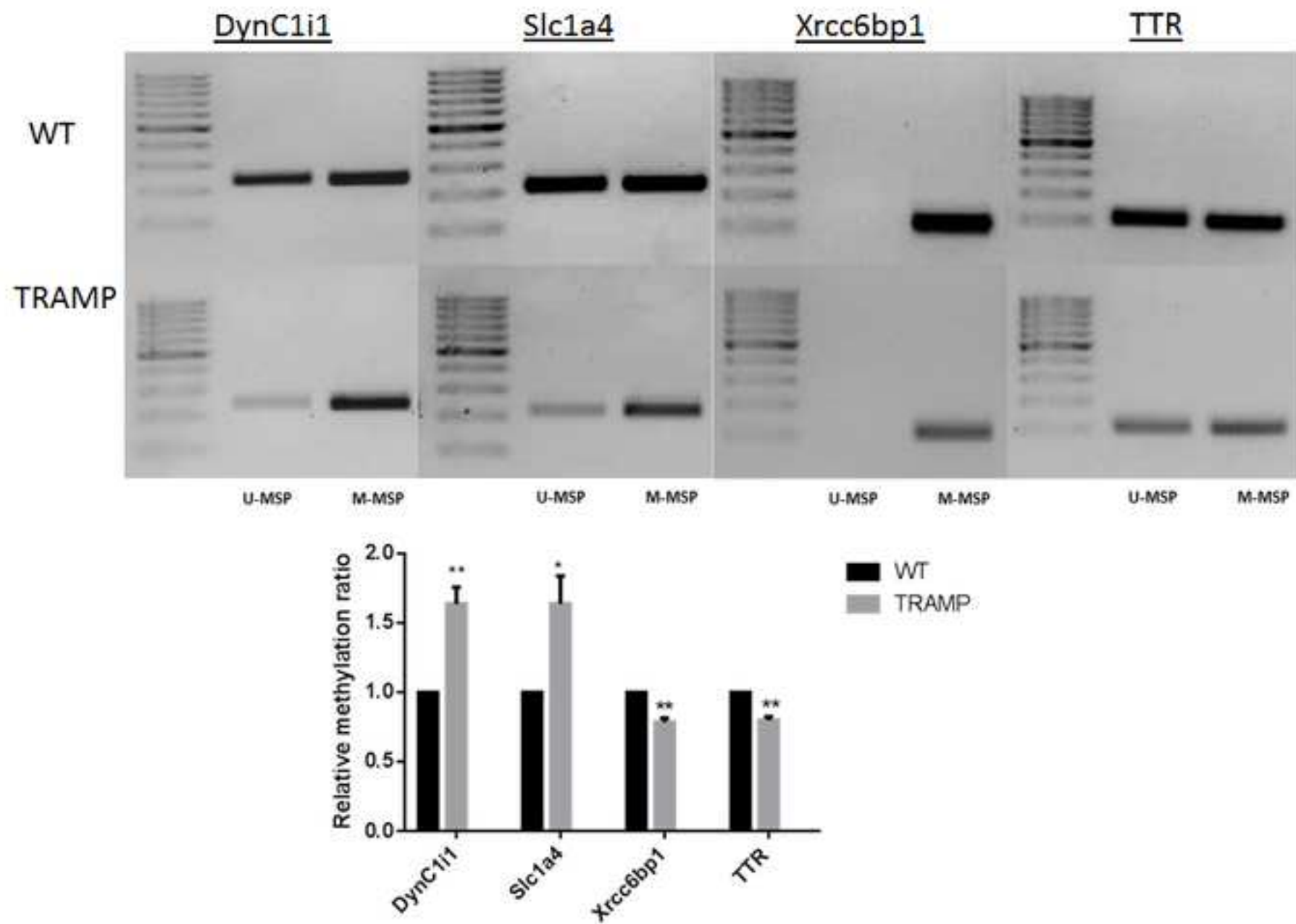
Table 7

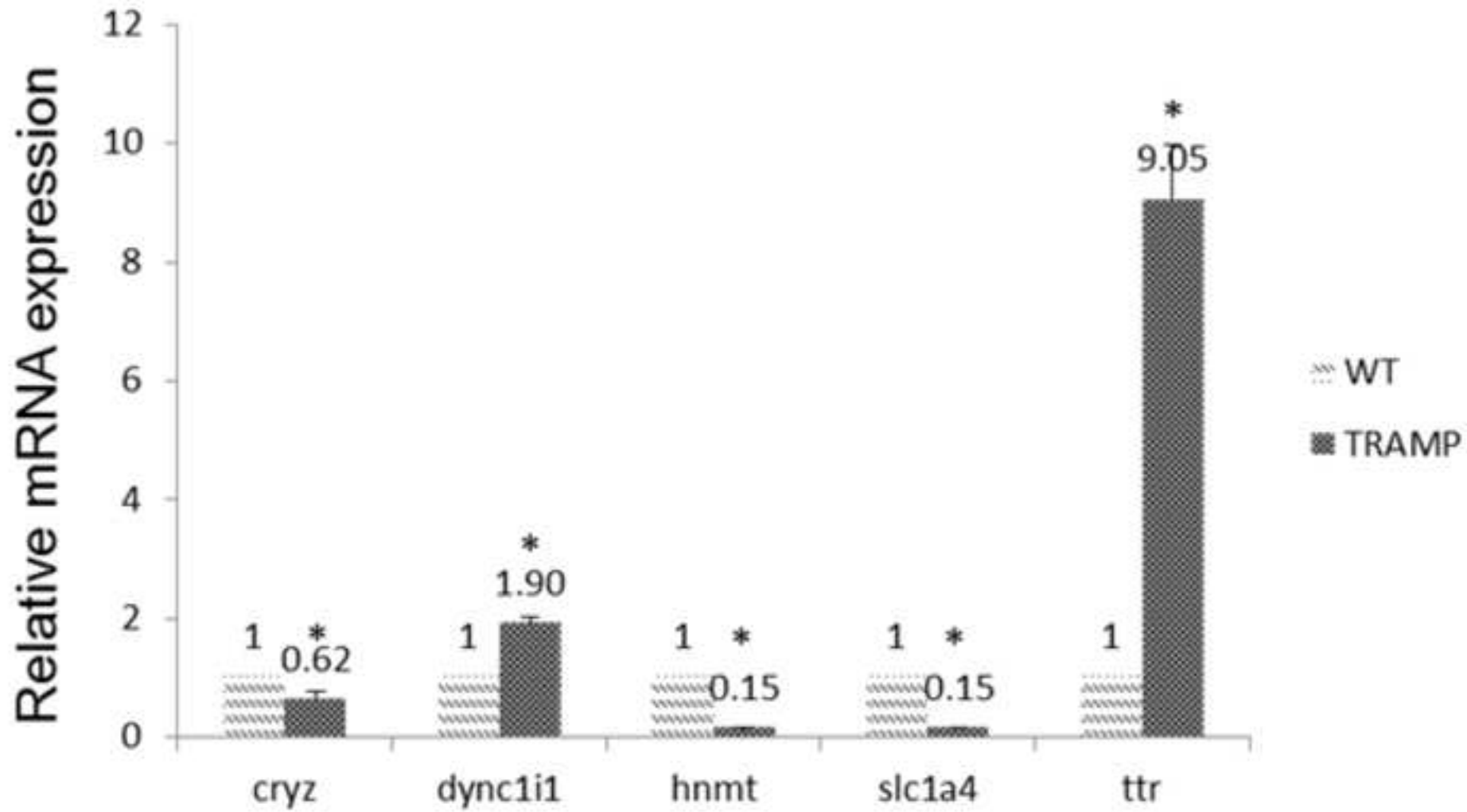
Altered methylation genes mapped to the neuropathic pain signaling pathway by IPA

Symbol	Gene Name	Log <sub>2</sub> -Fold Change	Type(s)
<b>GRM3</b>	glutamate receptor, metabotropic 3	-3.636	G-protein-coupled receptor
<b>GRIA1</b>	glutamate receptor, ionotropic, AMPA 1	-3.167	ion channel
<b>BDNF</b>	brain-derived neurotrophic factor	-2.373	growth factor
<b>CREB1</b>	cAMP-responsive element-binding protein 1	-2.274	transcription regulator
<b>GRM7</b>	glutamate receptor, metabotropic 7	-2.274	G-protein-coupled receptor
<b>GRIN3A</b>	glutamate receptor, ionotropic, N-methyl-D-aspartate 3A	-2.129	ion channel
<b>MAPK1</b>	mitogen-activated protein kinase 1	2.048	kinase
<b>TAC1</b>	tachykinin, precursor 1	2.408	other
<b>CAMK1</b>	calcium/calmodulin-dependent protein kinase ID	2.855	kinase
<b>D</b>			
<b>TACR1</b>	tachykinin receptor 1	2.855	G-protein-coupled receptor
<b>KCNN3</b>	potassium intermediate/small conductance calcium-activated channel, subfamily N, member 3	3.119	ion channel
<b>GPR37</b>	G protein-coupled receptor 37 (endothelin receptor type B-like)	3.855	G-protein-coupled receptor

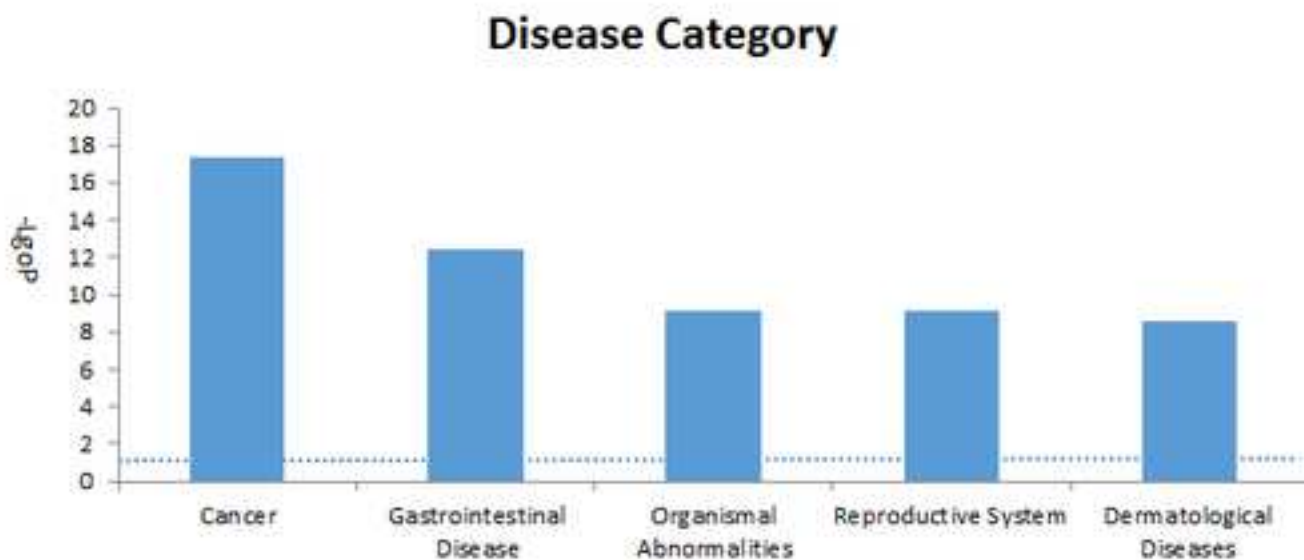
**A.****B.**



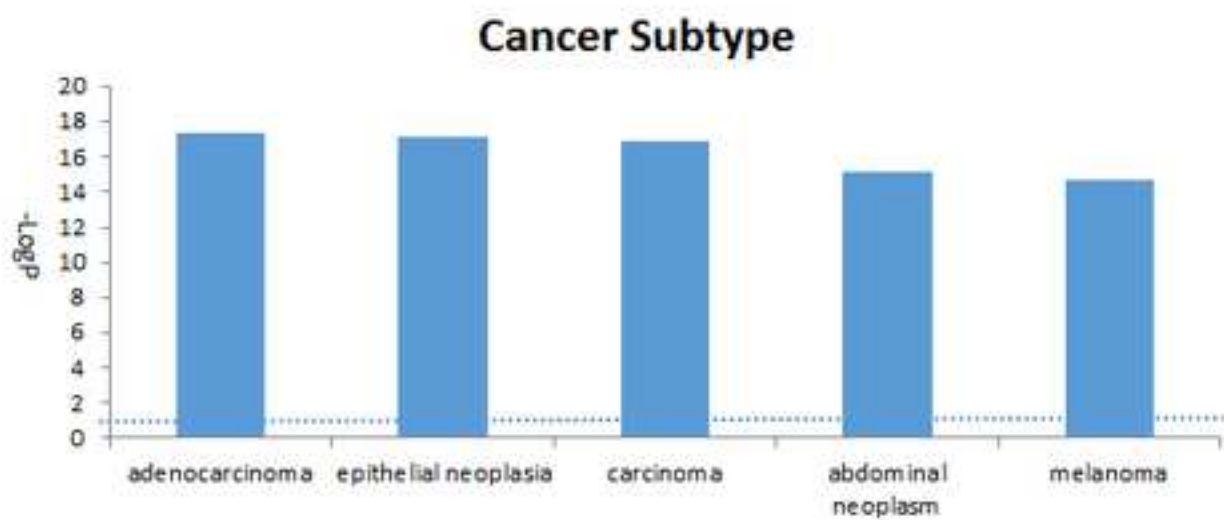




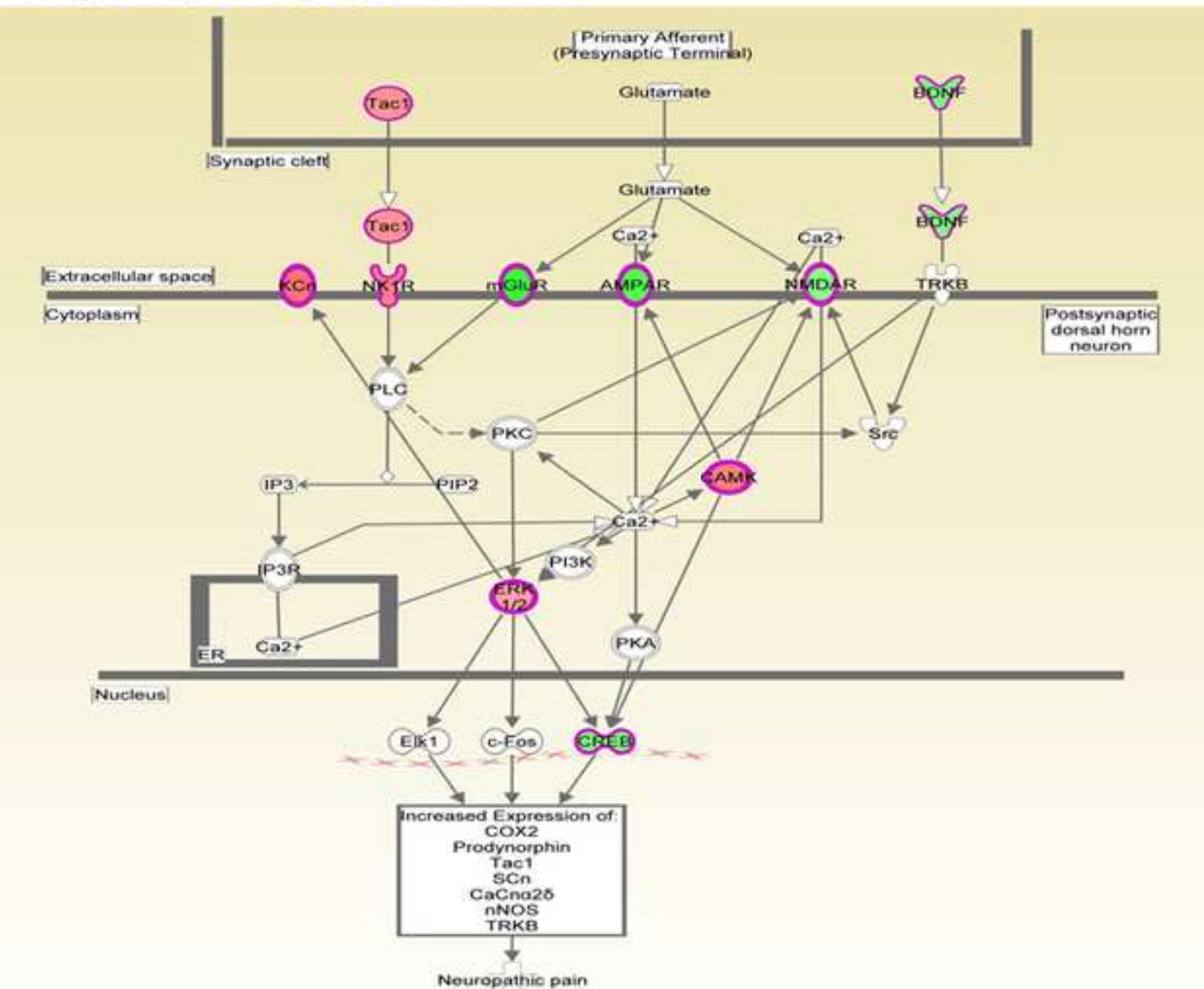
A



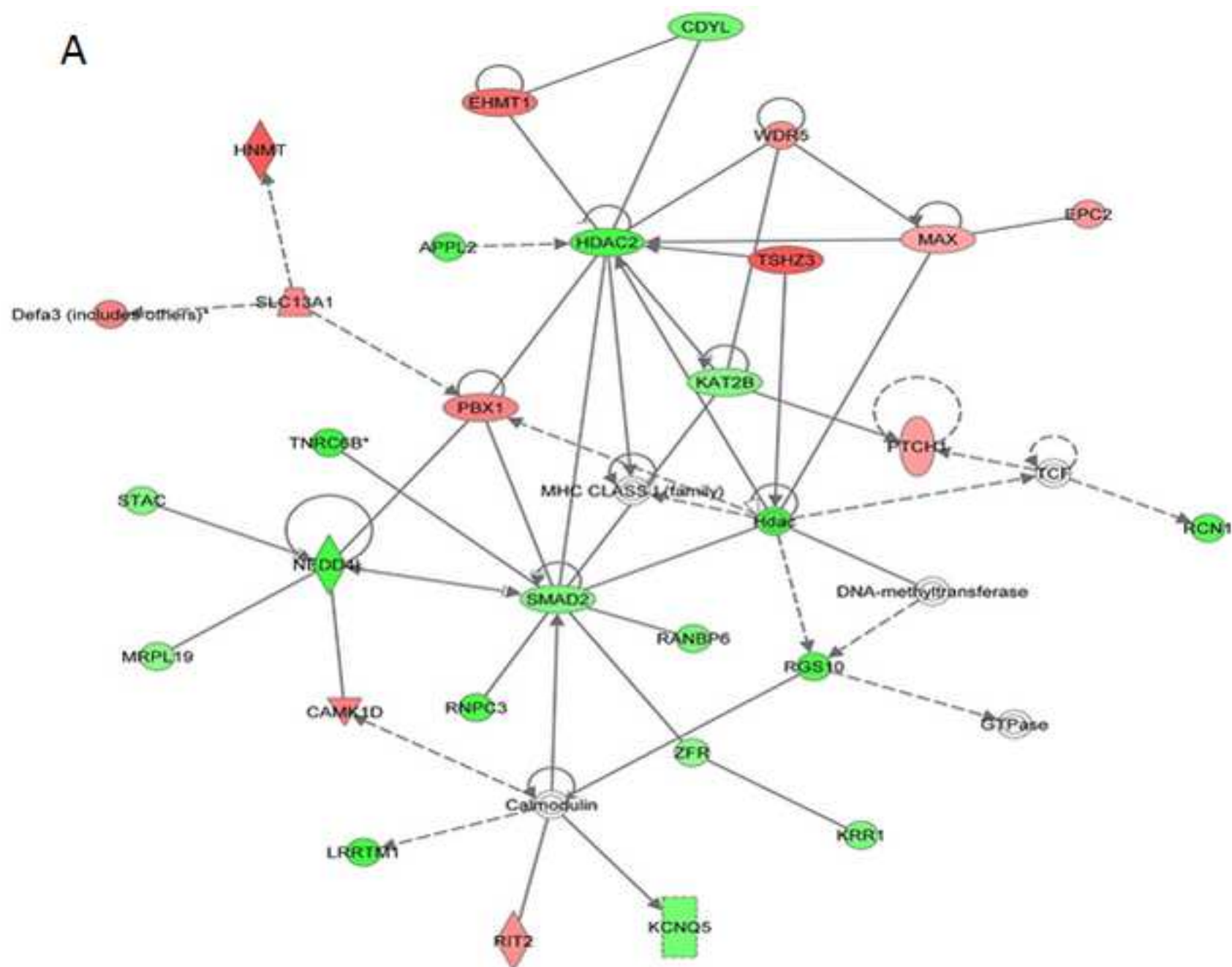
B

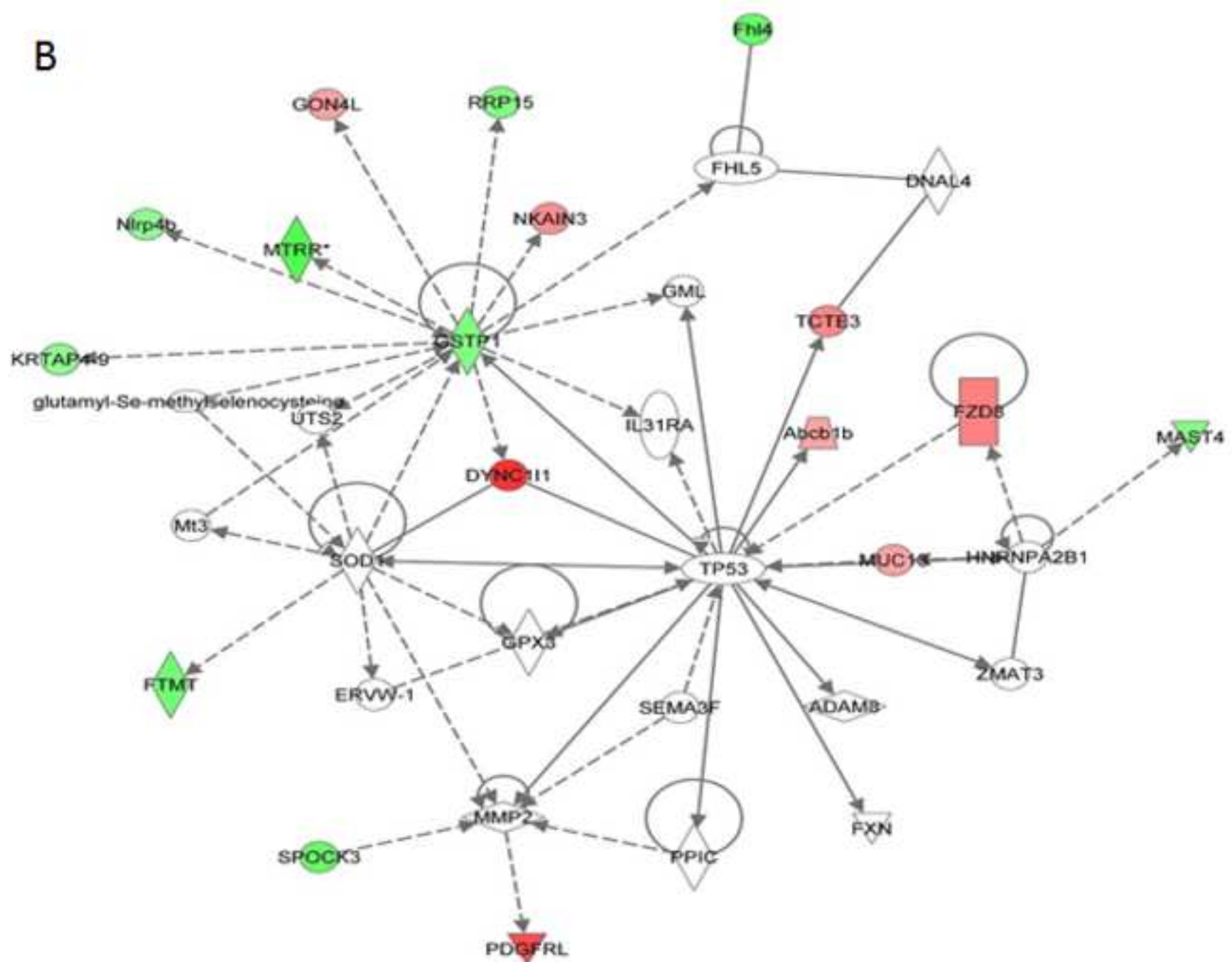


## Path Designer Neuropathic Pain Signaling In Dorsal Horn Neurons



A





C

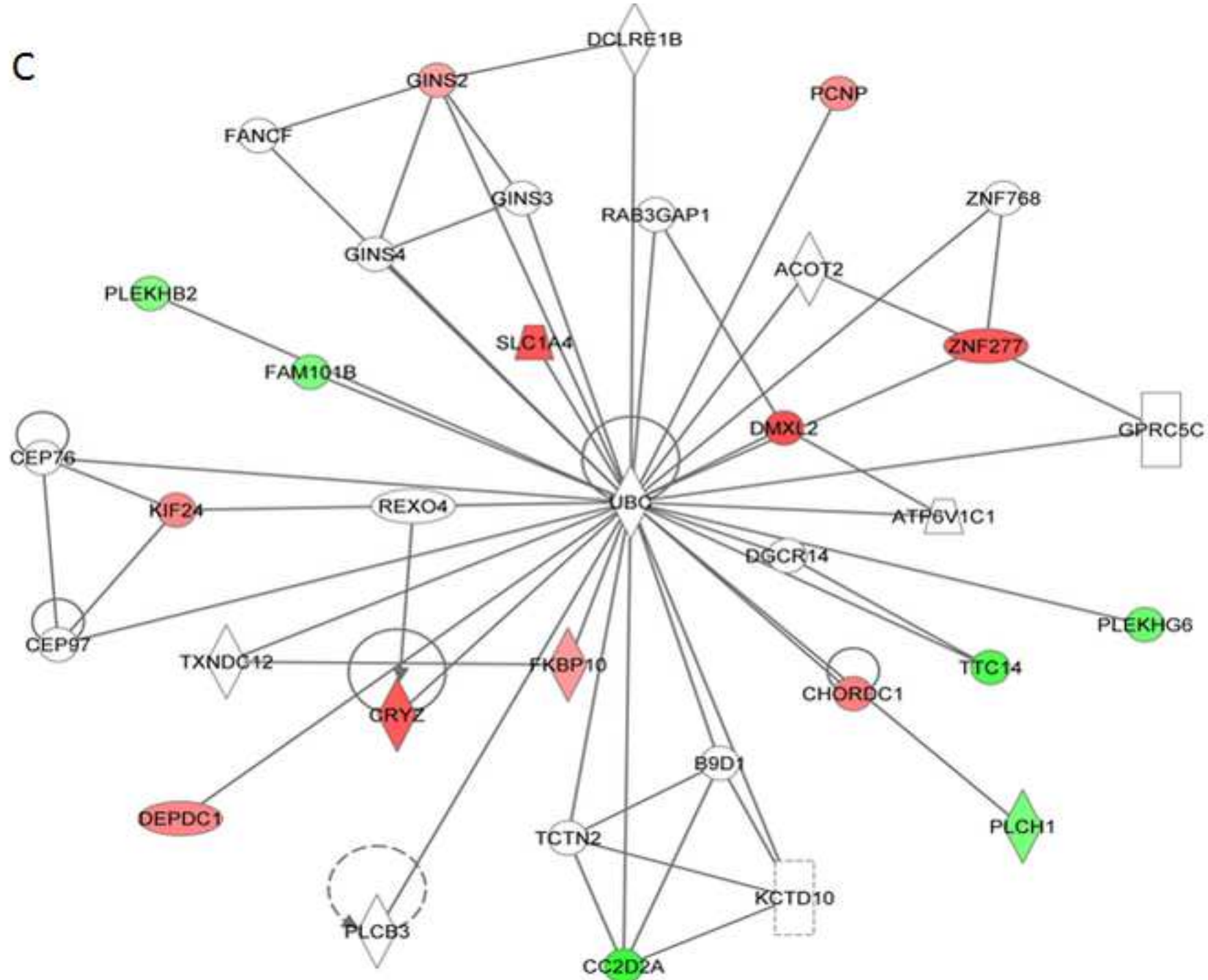


Fig 8

[Click here to download Figure figure-8.tif](#)

